CAPITAL UNIVERSITY OF SCIENCE AND TECHNOLOGY, ISLAMABAD

MHD Boundary Layer Flow Subjected to Joule Heating and Activation Energy over a Stretching/Shrinking Sheet

by

Haris Saleem

A thesis submitted in partial fulfillment for the degree of Master of Philosophy

in the

Faculty of Computing
Department of Mathematics

2021

I dedicate this dissertation to my family and friends. A special feeling of gratitude to my loving parents who have supported me in my studies.

CERTIFICATE OF APPROVAL

MHD Boundary Layer Flow Subjected to Joule Heating and Activation Energy over a Stretching/Shrinking Sheet

by

Haris Saleem

(MMT183006)

THESIS EXAMINING COMMITTEE

(a)	External Examiner	Dr. Taimoor Salahuddin	MUST, Mirpur, AK
(b)	Internal Examiner	Dr. Shafqat Hussain	CUST, Islamabad
(c)	Supervisor	Dr. Muhammad Sagheer	CUST, Islamabad

Dr. Muhammad Sagheer
Thesis Supervisor
December, 2021

Dr. Muhammad Sagheer
Head
Dept. of Mathematics
December, 2021

Dr. Muhammad Abdul Qadir
Dean
Faculty of Computing
December, 2021

Author's Declaration

I, **Haris Saleem**, hereby state that my M.Phil thesis titled "**MHD Boundary Layer Flow Subjected to Joule Heating and Activation Energy over a Stretching/Shrinking Sheet**" is my own work and has not been submitted previously by me for taking any degree from Capital University of Science and Technology, Islamabad or anywhere else in the country/abroad.

At any time if my statement is found to be incorrect even after my graduation, the University has the right to withdraw my M.Phil Degree.

(Haris Saleem)

Registration No: MMT183006

Plagiarism Undertaking

I solemnly declare that research work presented in this thesis titled "**MHD Boundary Layer Flow Subjected to Joule Heating and Activation Energy over a Stretching/Shrinking Sheet**" is solely my research work with no significant contribution from any other person. Small contribution/help wherever taken has been dully acknowledged and that complete thesis has been written by me.

I understand the zero tolerance policy of the HEC and Capital University of Science and Technology towards plagiarism. Therefore, I as an author of the above titled thesis declare that no portion of my thesis has been plagiarized and any material used as reference is properly referred/cited.

I undertake that if I am found guilty of any formal plagiarism in the above titled thesis even after award of M.Phil Degree, the University reserves the right to withdraw/revoke my M.Phil degree and that HEC and the University have the right to publish my name on the HEC/University website on which names of students are placed who submitted plagiarized work.

(Haris Saleem)
Registration No: MMT183006

Acknowledgement

All the appreciations are for **ALLAH** who is ever most lasting and sustainer of this universe. Everything belongs to him whatever is in the havens and whatever on the earth. Countless respect and endurance for **Prophet Muhammad (Peace be upon him)** the fortune of knowledge, who took the humanity out of ignorance and shows the right path.

I would first like to thank to my thesis supervisor **Dr. Muhammad Sagheer**, the Head of the Department of Mathematics, who helped me to solve and analyze the problem. The doors towards the supervisor were always open whenever I ran into a trouble spot or had a question about my research and writing. He consistently steered me in the right direction whenever he thought I needed it. I deem it my privilege to work under his able guidance. Also special thanks to **Dr. Shafqat Hussain** who also helped several times and all other faculty members.

A bundle of thanks are also fo my parents who always prayed and financially assisted me for my achievements.

(Haris Saleem)

Abstract

An effort is made to obtain the numerical solution of the boundary layer flow with Joule heating and activation energy over the stretching/shrinking sheet. The governing partial differential equations are reduced to a system of ordinary differential equations using suitable transformations. The resulting coupled system subject to the boundary conditions is solved using the shooting method. The influence of physical parameters such as magnetic field parameters, heat source parameter, Prandtl number, suction parameter, stretching/shrinking parameter, Eckert number, Schmidt number, thermophoresis parameter, Brownian motion, reaction parameter and temperature difference on the velocity profile, the temperature distribution, the concentration profile, skin friction coefficient, Nusselt number and Sherwood number are studied and presented in graphical and tabular forms. It is observed, that by raising the values of activation energy parameter, the numerical values of Nusselt number increase, and the concentration profile also increases. By raising the values of reaction rate parameter, Nusselt number will be decreased but Sherwood number shows increasing behaviour.

Contents

List of Figures

List of Tables

Abbreviations

IVPs	Initial Values Problems
MHD	Magnetohydrodynamics
ODEs	Orineary Differential Equations
PDEs	Partial Differential Equations
RK	Runge-Kutta

Symbols

μ	Viscosity
ρ	Density
ν	Kinematic viscosity
τ	Stress tensor
α	Thermal diffisuitivity
σ	Electrical conductivity
u	x-component of fluid velocity
v	y-component of fluid velocity
B_0	Magnetic field constant
k	Thermal conductivity of the fluid
a	Stretching constant
T_w	Temperature of the wall
T_∞	Ambient temperature of the fluid
T	Temperature
q_w	Heat flux at the surface
D	Positive constant
C_p	Specific heat at constant pressure
ψ	Stream function
ζ	Similarity variable
C_f	Skin friction coefficient
Nu	Nusselt number
Nu_x	Local Nusselt number
Sh	Sherwood number

Sh_x	Local Sherwood number
Re	Reynolds number
Re_x	Local Reynolds number
f	Dimensionless velocity
n	Heat flux parameter
M^2	Magnetic parameter
Sc	Schmidt number
Ec	Eckert number
Pr	Prandtl number
Q	Heat generation parameter
S	Suction parameter
Nb	Brownain motion parameter
Nt	Thermophoresis parameter
ϵ	Stretching/Shrinking parameter
B	Heat source parameter
θ	Dimensionless temperature
ϕ	Dimensionless concentration
C_∞	Ambient concentration
C	Concentration
C_w	Concentration at the stretching surface
Kr	Reaction constant
m	Fitted rate constant
E_1	Activation energy variable
δ	Heat generation/absorption variable
σ^*	Chemical reaction parameter

Chapter 1

Introduction

A significant form of flow that occurs in civil engineering is boundary layer action over a continuously moving solid surface. The heat transfer due to a continuously stretching surface through an ambient fluid is one of the thrust areas of current research. The problem of heat transfer are discussed in a broader spectrum of science and engineering operations, especially in chemical operations. Many chemical engineering operations, such as metallurgical processes and polymer extrusion, make the cooling of a molten liquid mandatory that has been stretched into a cooling system.

Sakiadis [1] was first who initiated the problem of boundary layer approximation over a stretching surface. He analyzed the non-Newtonian Maxwell fluid with nano materials over an exponentially stretched surface. The flow caused by the stretching sheet was investigated by Crane [2]. He examined the behaviour of boundary layer on the continuous surface. Chakrabarti and Gupta [3] investigated the linear stretching problem for hydromagnetic case. The variable-effects of surface temperature and heat flux on heat- transfer properties of a continuous stretching surface studied by Chen et al [4].

In recent time, numerious research articles such as [5], [6] and [7], are produced investigating the phenomenon of the fluid flow through stretching surface. They analyzed the impact of magnetic field parameter observing a reduction in the velocity of the fluid. The fluids play a vital role in heat transfer. Suction or injection

of a thermal boundary layer on a power law extended surface was investigated by Ali [8].

Heat transfer over a stretching surface with variable surface heat flux and uniform surface heat flux subject to injection and suction was examined by Elbashbeshy [9]. The boundary layer flows over a stretched impermeable wall are solved by means of an analytic technique, namely the homotopy analysis method was investigated by Liao [10]. The coupled fluid flow, heat and mass transfer phenomena over a stretching sheet with nonlinear velocity for micropolar fluid was studied by Bhargava et al. [11].

Khedr et al. [12] studied about the MHD flow of a micropolar fluid past a stretched permeable surface with heat generation or absorption. Effects of dissipation on nonlinear MHD flow over a stretching surface with a constant heat flux was examined by Devi and Ganga [13]. In a porous medium, radiant MHD flow over a non-isothermal stretching layer was investigated by Vyas and Srivastava [14]. The exact solution for axisymmetric flow and heat transfer over a radially stretching nonlinear layer investigated by Shahzad et al. [15].

The problem in opposite case of stretching sheet, a little bit known about the shrinking sheet having velocity on the boundary towards origin. The sheet is shrunk into a slot in this flow arrangement, and the flow differ from the stretching out scenario. It is also shown that maintaining flow over a shrinking sheet necessitates mass suction. According to a review of the literature, the flow generated by a shrinking sheet has earlier drew the attention of the modern-researchers due to its generated characteristics.

A shrinking sheet is a surface that has shrunk in size to a specific area due to external heat or suction. Shrinking film is one of the most popular applications of shrinking sheet problems in industries and engineering. Shrinking film is very useful in bulk product packaging because it can be easily unwrapped with enough heat. Shrinking can be used to investigate capillary effects in smaller pores, shrink-swell behaviour, and the hydraulic properties of agricultural clay soils. The presence and uniqueness of a similarity solution to the equation for flow caused by a shrinking sheet with suction was established by Miklavcic and Wang [16].

Sajid et al. [17] analyzed the MHD rotating flow of a viscous fluid over a shrinking surface. Closed form exact solution of MHD viscous flow over a shrinking sheet was examined by Fang and Zhang [18] in the absence of the heat transfer. The application of homotopy analysis method for MHD viscous flow over a shrinking sheet was examined by Sajid and Hayat [19]. An empirical solution for thermal boundary layer flow over a shrinking sheet with a specified wall temperature and a prescribed wall heat flux was examined by Fang and Zhang [20].

Hayat et al. [21] investigated the analytical solution for a second-grade fluid shrinking flow in a rotating frame. MHD flow and heat transfer due to a permeable shrinking sheet of a viscous electrically conducting fluid with prescribed surface heat flux investigated by Ali et al. [22]. For MHD viscous flow due to shrinking sheet, a simple non-perturbative solution was obtained by Noor et al. [23]. The impact of heat source/sink on MHD flow and heat transfer over a shrinking sheet with mass suction for a constant surface temperature was investigated by Bhattacharyya [24]. Das [25] investigated the effects of partial slip on steady boundary layer stagnation point flow of an electrically conducting micropolar fluid impinging normally towards a shrinking sheet in the presence of a uniform transverse magnetic field.

In 1889, a Swedish Scientist (Svantae Arrhenious), introduced the term activation energy, defined as, the least amount of energy acquired to initiate the chemical reaction. Food preparation, chemical engineering, oil reservoir engineering, and oil emulsion are just some of the processes that involve mass transport with activation energy. An industrial appliance that involves chemical reactions, such as a reactor, and which is required to make the reaction more reactive in order to achieve the maximum output. On the boundary layer of flow, a chemical reaction with activation energy has been presented by Bestman [26]. Hamid and Khan [27] modeled and studied activation energy on Williamson nanofluid with binary chemical reaction variable and magnetic field impacts.

The results show that increasing the reaction rate, increases the heat transfer rate. It is found that temperature and thermal layer thickness are decreased for larger stratification, to inspect stagnation point flow of tangent hyperbolic liquid

by a stretched sheet, to investigate activation energy was studied by Hayat et al. [28].

There has been no contribution on steady, laminar, two-dimensional boundary layer MHD flow of a viscous, electrically conducting fluid with heat transfer across a stretching/shrinking sheet specified with changing heat flux in the presence of a magnetic field and uniform heat source. Suction is used to stretch and shrink the sheet.

1.1 Thesis Contributions

The present survey is focused on the numerical analysis of 2-D MHD flow fluid along a boundary layer equation with the stretching/shrinking parameter, Joule heating effect, thermophoresis diffusion, Brownian motion, chemical reaction rate and activation energy. The proposed PDEs are converted into system of ODEs by applying similarity transformations. Further, for finding the numerical results of obtained ODEs, shooting method is utilized. The numerically obtained results are computed by using MATLAB software packages. The impact of significant parameters on velocity distribution, temperature distribution, concentration distribution, skin friction and Nusselt number have been discussed through graphs and tables.

1.2 Layout of Thesis

A brief overview of the contents of the thesis is provided below.

Chapter 2 includes some basic definitions and terminologies, which are useful to understand the concepts discussed later on.

Chapter 3 provides the proposed analytical study of numerical simulation of

MHD boundary layer flow passing through stretching/shrinking sheet. The numerical results of the governing flow equations are derived by the shooting method.

Chapter 4 extends the flow model discussed in Chapter 3 by using the effect of Joule heating, thermophoresis diffusion, Brownian motion and chemical reaction.

Chapter 5 provides the concluding remarks of the thesis.

References used in the thesis are mentioned in **Biblography**.

Chapter 2

Preliminaries

This chapter is prepared to present basic definitions related to fluid mechanics including definitions of some dimensionless numbers and governing laws just for the description of flow analysis presented in this dissertation. An explanation of shooting method is also included in this chapter.

2.1 Some Basic Terminologies

Definition 2.1.1 (Fluid)

"A fluid is defined as a material that deforms continuously and permanently under the application of a shearing stress." [29]

Definition 2.1.2 (Fluid Mechanics)

"Fluid mechanics is defined as that branch of engineering-science which deals with the behavior of the fluid (liquids or gases) under the condition of rest and motion." [30]

Definition 2.1.3 (Fluid Dynamics)

"It deals with the relations between velocities, acceleration of fluid with force or

energy causing them." [30]

Definition 2.1.4 (Fluid Statics)

"The study of fluids at rest is called fluid statics. The study of incompressible fluid under static conditions is called hydrostatic and that dealing with the compressible static gases is termed as aerostatic." [30]

Definition 2.1.5 (Kinematic)

"It deals with the velocities, acceleration and the pattern flow of fluids only." [30]

Definition 2.1.6 (Viscosity)

"Viscosity is defined as the property of a fluid which offers resistance to the movement of one layer of fluid over another adjacent layer of the fluid. Mathematically,

$$\mu = \frac{\tau}{\frac{\partial u}{\partial y}},$$

where μ is viscosity coefficient, τ is shear stress and $\frac{\partial u}{\partial y}$ represents the rate of shear deformation." [31]

Definition 2.1.7 (Kinetic Viscosity)

"It is defined as the ratio between the dynamic viscosity and density of fluid. It is denoted by Greek symbol ν called **nu**. Mathematically,

$$\nu = \frac{\mu}{\rho}." \text{ [31]}$$

2.2 Types of Fluid

Definition 2.2.1 (Ideal Fluids)

"A fluid, which is incompressible and has no viscosity, is known as an ideal fluid.

Ideal fluid is only an imaginary fluid as all the fluids, which exist, have some viscosity." [31]

Definition 2.2.2 (Real Fluids)

"A fluid, which possesses viscosity, is known as a real fluid. In actual practice, all the fluids are real fluids." [31]

Definition 2.2.3 (Newtonian Fluids)

"A real fluid, in which the shear stress is directly proportional to the rate of shear strain (or velocity gradient), is known as a Newtonian fluid. Water, kerosine oil and air are examples of Newtonian fluids. " [31]

Definition 2.2.4 (Non-Newtonian Fluids)

"A real fluid in which the shear stress is not directly proportional to the rate of shear strain (or velocity gradient), is known as a non-Newtonian fluid. Mud, polymer solutions and blood are examples of Non-Newtonian fluids." [31]

Definition 2.2.5 (Hydrodynamics)

"The study of the motion of fluids that are practically incompressible such as liquids, especially water and gases at low speeds is usually referred to as hydrodynamics." [32]

Definition 2.2.6 (Magnetohydrodynamics)

"Magnetohydrodynamics (MHD) is concerned with the mutual interaction of fluid flow and magnetic fields. The fluids in question must be electrically conducting and non-magnetic, which limits us to liquid metals, hot ionized gases (plasmas) and strong electrolytes." [33]

2.3 Types of Flow

Definition 2.3.1 (Rotational Flow)

"A flow is said to be rotational if the fluid particles while moving in direction of flow rotate about their mass centers. Flow near the solid boundaries is rotational, for example, motion of liquid in a rotating tank." [30]

Definition 2.3.2 (Irrotational Flow)

"A flow is said to be irrotational if the fluid particles while moving in the direction of flow do not rotate about their mass centers. Flow outside the boundary layer is generally considered irrotational." [30]

Definition 2.3.3 (Compressible Flow)

"It is that type of flow in which the density (ρ) of the fluid changes from point to point or in other words the density is not constant for the fluid flow. Mathematically,

$$\rho \neq b,$$

where b is constant." [30]

Definition 2.3.4 (Incompressible Flow)

"It is that type of flow in which the density is constant for the fluid flow. Liquids are generally incompressible while gases are compressible. Mathematically,

$$\rho = b,$$

where b is constant." [30]

Definition 2.3.5 (Steady Flow)

"The type of flow in which the fluid characteristics like, velocity, pressure, density

etc at a point do not change with time is called steady flow. Mathematically,

$$\frac{\partial P}{\partial t} = 0,$$

where P is any fluid property." [30]

Definition 2.3.6 (Unsteady Flow)

"It is that type of flow in which the velocity, pressure, density etc at any point change with respect to time. Mathematically,

$$\frac{\partial P}{\partial t} \neq 0,$$

where P is any fluid property." [30]

Definition 2.3.7 (Laminar Flow)

"A laminar flow is one in which path taken by the individual particles do not cross one another and move along well defined path. This type of flow is also called stream line flow or viscous flow, for example, blood in veins." [30]

Definition 2.3.8 (Turbulent Flow)

"A turbulent flow is that flow in which fluid particles move in a zig zag way, for example, high velocity flow in conduit of large size." [30]

2.4 Modes of Heat Transfer

Definition 2.4.1 (Heat Transfer)

"Heat transfer is a branch of engineering that deals with the transfer of thermal energy from one point to another within a medium or from one medium to another due to the occurrence of a temperature difference." [34]

Definition 2.4.2 (Conduction)

"The transfer of heat within a medium due to a diffusion process is called conduction." [34]

Definition 2.4.3 (Convection)

"Convection heat transfer is usually defined as energy transport affected by the motion of a fluid. The convection heat transfer between two dissimilar media is governed by Newton's law of cooling." [34]

Definition 2.4.4 (Forced convection)

"Forced convection heat transfer is induced by forcing a liquid or gas, over a hot body or surface." [35]

Definition 2.4.5 (Natural convection)

"Natural convection is generated by the density difference induced by the temperature differences within a fluid system and the small density variations present in these types of flows." [35]

Definition 2.4.6 (Thermal Conductivity)

"The Fourier heat conduction law states that the heat flow is proportional to the temperature gradient. The coefficient of proportionality is a material parameter known as the thermal conductivity which may be a function a number of variables." [34]

Definition 2.4.7 (Radiation)

"Radiation is the energy transfer due to the release of photons or electromagnetic waves from a surface volume. Radiation does not require any medium to transfer heat. The energy produced by radiation is transformed by electromagnetic waves." [36]

Definition 2.4.8 (Boundary layer)

"Viscous effects are particularly important near the solid surfaces, where the strong interaction of the molecules of the fluid with molecules of the solid causes the relative velocity between the fluid and the solid to become almost exactly zero for a stationary surface. Therefore, the fluid velocity in the region near the wall must reduce to zero. This is called no slip condition. In that condition there is no relative motion between the fluid and the solid surface at their point of contact. It follows that the flow velocity varies with distance from the wall; from zero at the wall to its full value some distance away, so that significant velocity gradients are established close to the wall. In most cases this region is thin (compared to the typical body dimension), and it is called a boundary layer." [29]

Definition 2.4.8 (Thermophoresis Diffusion)

"In a temperature gradient, small particles are pushed towards the lower temperature because of the asymmetry of molecular impacts. The resulting force which drives the particles along a temperature gradient towards the lower temperature, is called thermophoretic force and the mechanism thermophoresis." [29]

2.5 Dimensionless Numbers

Definition 2.5.1 (Eckert Number)

"It is a dimensionless number used in continuum mechanics. It describes the relation between flows and the boundary layer enthalpy difference and it is used for characterized heat dissipation. Mathematically,

$$Ec = \frac{u^2}{C_p \nabla T},$$

where C_p denotes the specific heat." [36]

Definition 2.5.2 (Prandtl Number)

"It is ratio between the momentum diffusivity ν and thermal diffusivity α. Mathematically, it can be defined as

$$Pr = \frac{\nu}{\alpha} = \frac{\frac{\mu}{\rho}}{\frac{k}{C_p \rho}} = \frac{\mu C_p}{k},$$

where μ represents the dynamic viscosity, Cp denotes the specific heat and k stands for thermal conductivity. The relative thickness of thermal and momentum boundary layer is controlled by Prandtl number. For small Pr, heat distributed rapidly corresponds to the momentum." [36]

Definition 2.5.3 (Skin Friction Coefficient)

"It is a dimensionless number and is defined as

$$C_{f_x} = \frac{2\tau_0}{\rho u_w^2},$$

where τ_0 is the local wall shear stress, ρ is the fluid density and u is the free stream velocity. It expresses the dynamic friction resistance originating in viscous fluid flow around a fixed wall." [37]

Definition 2.5.4 (Nusselt Number)

"It is the ratio of the convective to the conductive heat transfer at a boundary in a fluid. Mathematically,

$$Nu_x = \frac{hL}{k},$$

where h stands for the convection heat transfer, L for the characteristic length and k stands for thermal conductivity." [35]

Definition 2.5.5 (Sherwood Number)

"It is a nondimensional quantity which shows the ratio of the mass transport by

convection to the transfer of mass by diffusion. Mathematically,

$$Sh_x = \frac{kL}{D},$$

where L is the characteristic length, D is the mass diffusivity and k is the mass transfer coeffcient." [38]

Definition 2.5.6 (Reynolds Number)

"It is defined as the ratio of inertia force of a flowing fluid and the viscous force of the fluid. Mathematically,

$$Re = \frac{U_w L}{\nu},$$

where U_w denotes the free stream velocity, L is the characteristic length and ν stands for kinematic viscosity." [31]

2.6 Governing Laws

Definition 2.6.1 (Continuity Equation)

"The principle of conservation of mass can be stated as the time rate of change of mass is fixed volume is equal to the net rate of flow of mass across the surface. Mathematically, it can be written as

$$\frac{\partial \rho}{\partial t} + \nabla.(\rho \mathbf{u}) = 0." \text{ [34]}$$

Definition 2.6.2 (Momentum Equation)

"The momentum equation states that the time rate of change of linear momentum of a given set of particles is equal to the vector sum of all the external forces acting on the particles of the set, provided Newtons Third Law of action and reaction

governs the internal forces. Mathematically, it can be written as:

$$\frac{\partial}{\partial t}(\rho \mathbf{u}) + \nabla.[(\rho \mathbf{u})\mathbf{u}] = \nabla.\mathbf{T} + \rho g." \text{ [34]}$$

Definition 2.6.3 (Energy Equation)

"Energy can neither created nor destroyed, it can be transformed from one form to another form but total amount of an isolated system remains constant. For example energy is conserved over time. It is the fundamental law of physics which is also known as the first law of thermodynamics.

The mathematical form of energy equation in two-dimensional for fluid can be written as,

$$\frac{\partial T}{\partial x} + v\frac{\partial T}{\partial y} = \alpha\left[\frac{\partial^2 T}{\partial x^2} + \frac{\partial^2 T}{\partial y^2}\right] + \frac{\mu}{\rho C_p}\phi^*,$$

where ϕ^* is the dissipation function." [34]

2.7 Shooting Method

"To elaborate the shooting method, consider the following nonlinear boundary value problem.

$$\left.\begin{aligned} &2f'''(x) + f(x)f''(x) = 0. \\ &f(0) = 0, \quad f'(0) = 0, \quad f'(G) = 1. \end{aligned}\right\} \tag{2.1}$$

To reduce the order of the above boundary value problem, introduce the following notations.

$$f = y_1 \qquad f' = y_1' = y_2 \qquad f'' = y_2' = y_3 \qquad f''' = y_3'. \tag{2.2}$$

As a result, (2.1) converted into the system of first order ODEs.

$$y_1' = y_2, \qquad y_1(0) = 0, \tag{2.3}$$

$$y_2' = y_3, \qquad y_2(0) = 0, \tag{2.4}$$

$$y_3' = -\frac{1}{2} y_1 y_3, \qquad y_3(0) = w, \tag{2.5}$$

where w is the missing initial condition which will be guessed.

The above IVP will be numerically solved by the RK-4 method. The missing condition w is to be chosen such that.

$$y_2(G, w) = 1. \tag{2.6}$$

For convenience, now onward, $y_2(G, w)$ will be denoted by $y_2(w)$.

Let us further denote $y_2(w) - 1$ by $H(w)$, so that

$$H(w) = 0. \tag{2.7}$$

The above equation can be solved by using Newton's method, which has the following iterative formula.

$$w^{n+1} = w^n - \frac{H(w^n)}{\frac{\partial H(w^n)}{\partial w}}, \qquad n = 0, 1, 2...$$

or

$$w^{n+1} = w^n - \frac{y_2(w^n) - 1}{\frac{\partial y_2(w^n)}{\partial w}}. \qquad n = 0, 1, 2... \tag{2.8}$$

To find $\frac{\partial y_2(w^n)}{\partial w}$, introduce the following notations.

$$\frac{\partial y_1}{\partial w} = y_4, \quad \frac{\partial y_2}{\partial w} = y_5, \quad \frac{\partial y_3}{\partial w} = y_6. \tag{2.9}$$

As a result of these new notations, the Newton's iterative scheme, will then get the following form.

$$w^{n+1} = w^n - \frac{y_2(w^n) - 1}{y_5(w^n)}. \tag{2.10}$$

Now differentiating the system of two first order ODEs (2.3)-(2.5) with respect to w, we get another system of ODEs, as follows.

$$y_4' = y_5, \qquad y_4(0) = 0. \tag{2.11}$$

$$y_5' = y_6, \qquad y_5(0) = 0. \tag{2.12}$$

$$y_6' = -\frac{1}{2}\left[y_1 y_6 + y_3 y_4\right], \qquad y_6(0) = 1. \tag{2.13}$$

Writing all the six ODEs (2.3), (2.4), (2.5), (2.11), (2.12) and (2.13) together, we have the following initial value problem.

$$\begin{aligned}
y_1' &= y_2, & y_1(0) &= 0.\\
y_2' &= y_3, & y_2(0) &= 0.\\
y_3' &= -\frac{1}{2} y_1 y_3, & y_3(0) &= w.\\
y_4' &= y_5, & y_4(0) &= 0.\\
y_5' &= y_6, & y_5(0) &= 0.\\
y_6' &= -\frac{1}{2}\left[y_1 y_6 + y_3 y_4\right], & y_6(0) &= 1.
\end{aligned}$$

The above system together will be solved numerically by Runge-Kutta method of order four. The missing condition will be updated by the Newton's formula in (2.10).

The stopping criteria for the Newton's technique is set as,

$$\mid y_2(w) - 1 \mid < \epsilon,$$

where $\epsilon > 0$ is an arbitrarily small positive number."

Chapter 3

Numerical Study of a MHD Boundary Layer Flow

In this chapter, the numerical analysis of a 2-D MHD fluid flow past a linearly stretching/shrinking sheet under the influence of uniform magnetic field and heat generation will be carried out. The set of PDEs is converted into a system of dimensionless ODEs by an appropriate transformation. In order to solve ODEs, the shooting technique is implemented in MATLAB. At the end of this chapter the numerical solution of various profiles will be discussed. The obtained numerical results are given in the form of tables and graphs. This chapter provides a detailed review of [39].

3.1 Mathematical Modeling

Assume a steady, 2-D laminar flow of viscous, incompressible, electrically conducting fluid, caused by a stretching/shrinking sheet subjected to suction in the presence of uniform transverse magnetic field. A uniform magnetic field of strength B_0 is applied in the direction parallel to y-axis normal to the sheet lying horizontally along x-axis.

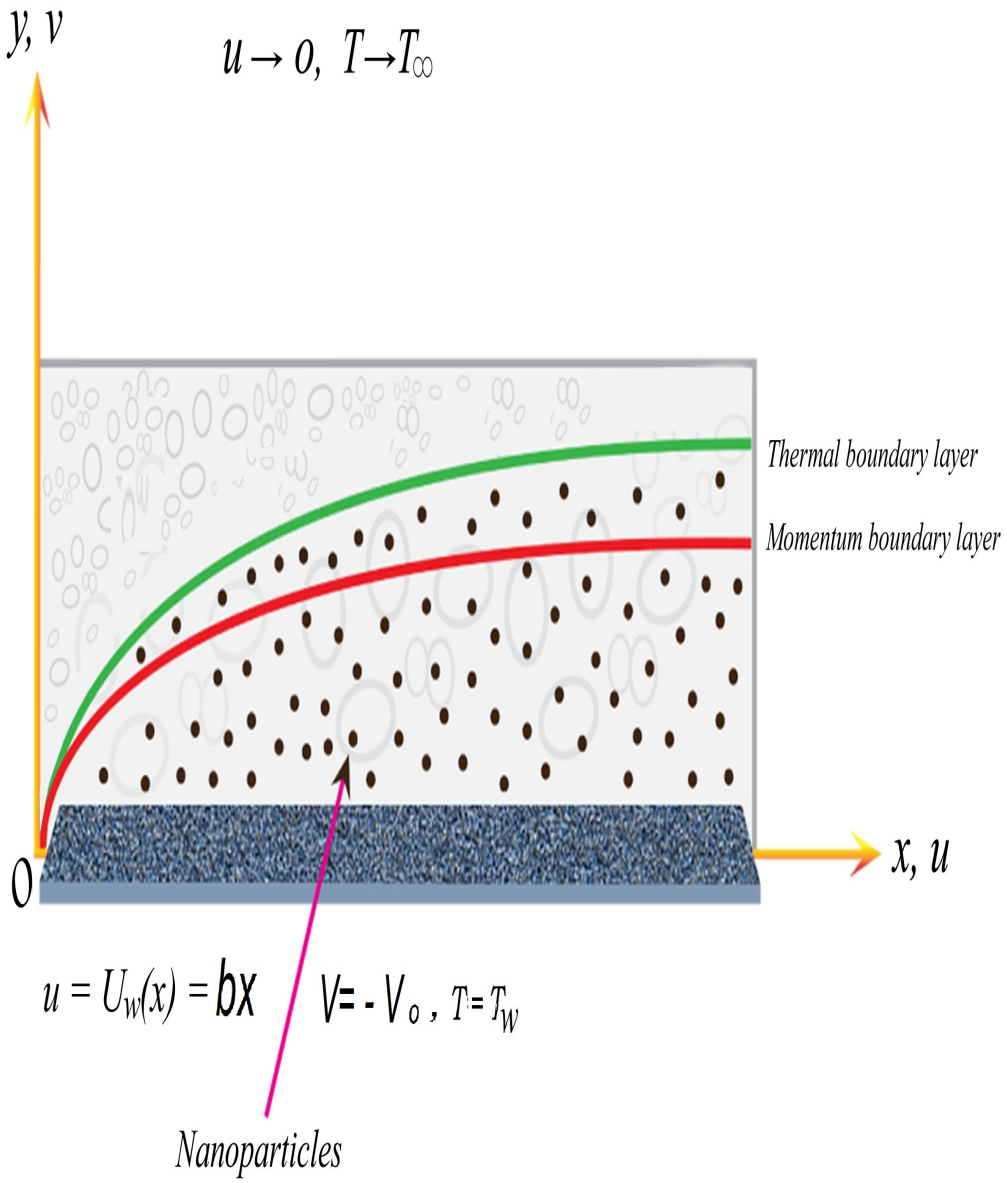

FIGURE 3.1: Systematic representation of physical model.

The set of equations describing the flow are as follows:

$$\frac{\partial u}{\partial x} + \frac{\partial v}{\partial y} = 0, \tag{3.1}$$

$$u\frac{\partial u}{\partial x} + v\frac{\partial u}{\partial y} = \nu\left(\frac{\partial^2 u}{\partial y^2}\right) - \frac{\sigma B_0^2}{\rho}u, \tag{3.2}$$

$$\rho C_p\left(u\frac{\partial T}{\partial x} + v\frac{\partial T}{\partial y}\right) = k\left(\frac{\partial^2 T}{\partial y^2}\right) + Q(T - T_\infty). \tag{3.3}$$

The associated BCs have been taken as:

$$\left.\begin{aligned} &U_w = u = bx, \quad v = -v_0, \quad -k\frac{\partial T}{\partial y} = q_w = Dx^n, \quad at \quad y = 0, \\ &u \to 0, \quad T \to T_\infty, \quad as \quad y \to \infty. \end{aligned}\right\} \tag{3.4}$$

The velocity component along x-axis and y-axis are denoted by u and v, ν denotes kinematic viscosity, the base fluid density is denoted by ρ, the specific heat capacity at constant pressure is denoted by C_p, thermal conductivity of the fluid is denoted by k, dimensional heat generation coefficient is denoted by Q, electrical conductivity of the fluid is denoted by σ.

For the conversion of the mathematical model (3.1)-(3.3) into the system of ODEs, the following similarity transformation can be considered [39].

$$\left.\begin{aligned} \psi(x,y) &= \sqrt{a\nu}xf(\zeta), \\ T - T_\infty &= \frac{Dx^n}{k}\sqrt{\frac{a}{\nu}}\theta(\zeta), \\ \zeta &= y\sqrt{\frac{a}{\nu}}, \end{aligned}\right\} \tag{3.5}$$

where ψ denotes the stream function.

The detailed procedure for the conversion of (3.1)-(3.3) into the dimensionless form has been described in the upcoming discussion:

- $$\begin{aligned} u &= \frac{\partial \psi}{\partial y} \\ &= \frac{\partial}{\partial y}\left(\sqrt{a\nu}xf(\zeta)\right) \\ &= \sqrt{a\nu}xf'(\zeta)\frac{\partial \zeta}{\partial y} \\ &= \sqrt{a\nu}xf'(\zeta)\sqrt{\frac{a}{\nu}} \\ u &= axf'(\zeta). \end{aligned} \tag{3.6}$$
- $$\begin{aligned} v &= -\frac{\partial \psi}{\partial x} \\ &= -\frac{\partial}{\partial x}\left(\sqrt{a\nu}xf(\zeta)\right) \end{aligned}$$

$$= -\sqrt{a\nu}\left(f(\zeta) + xf'(\zeta)\frac{\partial\zeta}{\partial x}\right)$$

$$v = -\sqrt{a\nu}f(\zeta). \tag{3.7}$$

- $$\frac{\partial u}{\partial x} = \frac{\partial}{\partial x}\left(af'(\zeta)x\right)$$
$$= a\left(f'(\zeta) + xf''(\zeta)\frac{\partial\zeta}{\partial x}\right)$$
$$= af'(\zeta). \tag{3.8}$$
- $$\frac{\partial u}{\partial y} = \frac{\partial}{\partial y}(axf'(\zeta))$$
$$= axf''(\zeta)\frac{\partial\zeta}{\partial y}$$
$$= a\sqrt{\frac{a}{\nu}}xf''(\zeta). \tag{3.9}$$
- $$\frac{\partial^2 u}{\partial y^2} = a\sqrt{\frac{a}{\nu}}xf'''(\zeta)\frac{\partial\zeta}{\partial y}$$
$$= a\sqrt{\frac{a}{\nu}}xf'''(\zeta)\sqrt{\frac{a}{\nu}}$$
$$= \frac{a^2}{\nu}xf'''(\zeta). \tag{3.10}$$
- $$\frac{\partial v}{\partial y} = \frac{\partial}{\partial y}\left(-\sqrt{a\nu}f(\zeta)\right)$$
$$= -\sqrt{a\nu}f'(\zeta)\frac{\partial\zeta}{\partial y}$$
$$= -\sqrt{a\nu}f'(\zeta)\sqrt{\frac{a}{\nu}}$$
$$= -af'(\zeta). \tag{3.11}$$
- $$T - T_\infty = \frac{Dx^n}{k}\sqrt{\frac{\nu}{a}}\theta(\zeta). \tag{3.12}$$

$$T = T_\infty + \frac{Dx^n}{k}\sqrt{\frac{\nu}{a}}\theta(\zeta)$$
$$\frac{\partial T}{\partial x} = \frac{D}{k}\sqrt{\frac{\nu}{a}}\left[nx^{n-1}\theta(\zeta)\right]$$
$$= \frac{nD}{k}\sqrt{\frac{\nu}{a}}x^{n-1}\theta(\zeta). \tag{3.13}$$

- $$\frac{\partial T}{\partial y} = \frac{Dx^n}{k}\sqrt{\frac{\nu}{a}}\theta'(\zeta)\frac{\partial\zeta}{\partial y}$$
$$= \frac{Dx^n}{k}\sqrt{\frac{\nu}{a}}\theta'(\zeta)\sqrt{\frac{a}{\nu}}$$
$$= \frac{Dx^n}{k}\theta'(\zeta). \tag{3.14}$$

- $$\frac{\partial^2 T}{\partial y^2} = \frac{D}{k}\sqrt{\frac{a}{\nu}}x^n\theta''(\zeta). \tag{3.15}$$
- $$u\frac{\partial u}{\partial x} = axf'(\zeta)\left(af'(\zeta)\right) = a^2xf'^2(\zeta). \tag{3.16}$$
- $$v\frac{\partial u}{\partial y} = -\sqrt{a\nu}f(\zeta)\left(a\sqrt{\frac{a}{\nu}}xf''(\zeta)\right) = a^2xf''(\zeta)f(\zeta). \tag{3.17}$$

Equation (3.1) is easily satisfied by using (3.8) and (3.11) as follows:

$$\begin{aligned}\frac{\partial u}{\partial x} + \frac{\partial v}{\partial y} &= af'(\zeta) - af'(\zeta)\\ \frac{\partial u}{\partial x} + \frac{\partial v}{\partial y} &= 0.\end{aligned} \tag{3.18}$$

Using (3.16) and (3.17), the left side of (3.2) becomes:

$$\begin{aligned}&u\frac{\partial u}{\partial x} + v\frac{\partial u}{\partial y}\\ &= a^2xf'^2(\zeta) - a^2xf''(\zeta)f(\zeta)\\ &= xa^2\left[f'^2(\zeta) - f''(\zeta)f(\zeta)\right].\end{aligned} \tag{3.19}$$

Using (3.6) and (3.10), the right side of (3.2) becomes:

$$\begin{aligned}&\nu\left(\frac{\partial^2 u}{\partial y^2}\right) - \frac{\sigma B_0^2}{\rho}u\\ &= \nu\left(\frac{a^2}{\nu}xf'''(\zeta)\right) - \frac{\sigma B_0^2}{\rho}axf'(\zeta)\\ &= xa^2\left[f'''(\zeta) - \frac{\sigma B_0^2}{a\rho}f'(\zeta)\right]\\ &= xa^2\left[f'''(\zeta) - M^2f'(\zeta)\right].\end{aligned} \tag{3.20}$$

Using (3.19) and (3.20), the dimensionless form of (3.2) can be seen as follows:

$$\left(u\frac{\partial u}{\partial x} + v\frac{\partial u}{\partial y}\right) = \nu\left(\frac{\partial^2 u}{\partial y^2}\right) - \frac{\sigma}{\rho}B_0^2u$$

$$\Rightarrow \quad xa^2\left[f'^2(\zeta) - f''(\zeta)f(\zeta)\right] = xa^2\left[f'''(\zeta) - M^2 f'(\zeta)\right].$$
$$\Rightarrow \quad f'^2(\zeta) - f''(\zeta)f(\zeta) = f'''(\zeta) - M^2 f'(\zeta).$$
$$\Rightarrow \quad f'''(\zeta) + f(\zeta)f''(\zeta) - f'^2(\zeta) - M^2 f'(\zeta) = 0. \tag{3.21}$$

Using (3.6), (3.7), (3.13) and (3.14), in the left side of (3.3), we get:

$$\begin{aligned} u\frac{\partial T}{\partial x} + v\frac{\partial T}{\partial y} &= axf'(\zeta)\left[\frac{nD}{k}\sqrt{\frac{\nu}{a}}x^{n-1}\theta(\zeta)\right] - \sqrt{\nu a}f(\zeta)\left[\frac{D}{k}x^n\theta'(\zeta)\right] \\ &= \frac{anD}{k}\sqrt{\frac{\nu}{a}}x^n f'(\zeta)\theta(\zeta) - \frac{D}{k}\sqrt{\nu a}x^n f(\zeta)\theta'(\zeta) \\ &= \frac{aD}{k}\sqrt{\frac{\nu}{a}}x^n\left[nf'(\zeta)\theta(\zeta) - f\theta'(\zeta)\right]. \end{aligned} \tag{3.22}$$

Using (3.12) and (3.15) in the right side of (3.3), we get the following:

$$\begin{aligned} \frac{k}{\rho C_p}\frac{\partial^2 T}{\partial y^2} + \frac{Q}{\rho C_p}(T - T_\infty) &= \frac{kD}{k\rho C_p}\sqrt{\frac{a}{\nu}}x^n\theta''(\zeta) + \frac{Q}{\rho C_p}\frac{Dx^n}{k}\sqrt{\frac{\nu}{a}}\theta(\zeta) \\ &= \frac{aD}{k}\sqrt{\frac{\nu}{a}}x^n\left[\frac{k}{\rho C_p \nu}\theta''(\zeta) + \frac{Q}{a\rho C_p}\theta(\zeta)\right]. \end{aligned} \tag{3.23}$$

With the help of (3.22) and (3.23), the following dimensionless form of (3.3), is obtained:

$$u\frac{\partial T}{\partial x} + v\frac{\partial T}{\partial y} = \frac{k}{\rho C_p}\frac{\partial^2 T}{\partial y^2} + \frac{Q}{\rho C_p}(T - T_\infty).$$
$$\Rightarrow \quad \frac{aD}{k}\sqrt{\frac{\nu}{a}}x^n\left[nf'(\zeta)\theta(\zeta) - f(\zeta)\theta'(\zeta)\right] = \frac{aD}{k}\sqrt{\frac{\nu}{a}}x^n\left[\frac{k}{\rho C_p\nu}\theta''(\zeta) + \frac{Q}{a\rho C_p}\theta(\zeta)\right].$$
$$\Rightarrow \quad nf'(\zeta)\theta(\zeta) - f(\zeta)\theta'(\zeta) = \frac{k}{\rho C_p\nu}\theta'' + \frac{Q}{a\rho C_p}\theta(\zeta).$$
$$\Rightarrow \quad nf'(\zeta)\theta(\zeta) - f(\zeta)\theta'(\zeta) = \frac{1}{Pr}\theta''(\zeta) + B\theta(\zeta).$$
$$\Rightarrow \quad \theta''(\zeta) + Pr\left[f(\zeta)\theta'(\zeta) - nf'(\zeta)\theta(\zeta) + B\theta(\zeta)\right] = 0. \tag{3.24}$$

The corresponding BCs are transformed into the non-dimensional form through the following procedure:

- $u = bx, \qquad at \quad y = 0.$

$$\Rightarrow \quad u = af'(\zeta)x, \qquad at \quad \zeta = 0.$$

$$\Rightarrow \quad af'(\zeta)x = bx, \qquad at \quad \zeta = 0.$$

$$\Rightarrow \quad f'(\zeta) = \epsilon, \qquad \epsilon = b/a, \qquad at \quad \zeta = 0.$$

$$\Rightarrow \quad f'(\zeta) = \epsilon, \qquad at \quad \zeta = 0.$$

- $v = -v_0, \qquad at \quad y = 0.$

$$\Rightarrow \quad v = -\sqrt{a\nu}f(\zeta), \qquad at \quad \zeta = 0.$$

$$\Rightarrow \quad -\sqrt{a\nu}f(\zeta) = -v_0, \qquad at \quad \zeta = 0.$$

$$\Rightarrow \quad f(\zeta) = \frac{v_0}{\sqrt{a\nu}}, \qquad at \quad \zeta = 0.$$

$$\Rightarrow \quad f(\zeta) = S, \qquad at \quad \zeta = 0.$$

- $-k\frac{\partial T}{\partial y} = Dx^n, \qquad at \quad y = 0.$

$$\Rightarrow \quad \frac{\partial T}{\partial y} = \frac{Dx^n}{k}\theta'(\zeta), \qquad at \quad \zeta = 0.$$

$$\Rightarrow \quad -k\left(\frac{Dx^n}{k}\theta'(\zeta)\right) = Dx^n, \qquad at \quad \zeta = 0.$$

$$\Rightarrow \quad \theta'(\zeta) = -1, \qquad at \quad \zeta = 0.$$

$$\Rightarrow \quad \theta'(\zeta) = -1, \qquad at \quad \zeta = 0.$$

- $u \to (0), \qquad as \quad y \to \infty.$

$$\Rightarrow \quad af'(\zeta)x \to (0), \qquad as \quad \zeta \to \infty.$$

$$\Rightarrow \quad f'(\zeta) \to (0), \qquad as \quad \zeta \to \infty.$$

$$\Rightarrow \quad f'(\zeta) \to (0), \qquad as \quad \zeta \to \infty.$$

- $T \to T_\infty, \qquad as \quad y \to \infty.$

$$\Rightarrow \quad T - T_\infty = \frac{Dx^n}{k}\sqrt{\frac{\nu}{a}}\theta(\zeta), \qquad as \quad \zeta \to \infty.$$

$$\Rightarrow \quad \theta(\zeta) \to 0, \qquad as \quad \zeta \to \infty.$$

The final dimensionless form of the governing model is:

$$f'''(\zeta) + f''(\zeta)f(\zeta) - f'^2(\zeta) - M^2 f'(\zeta) = 0, \tag{3.25}$$

$$\theta''(\zeta) + Pr\left[f(\zeta)\theta'(\zeta) - nf'(\zeta)\theta(\zeta) + B\theta(\zeta)\right] = 0. \tag{3.26}$$

The associated BCs (3.4) in the dimensionless form are as follows:

$$\left.\begin{aligned} f(0) = S, \quad f'(0) = \epsilon, \quad \theta'(0) = -1. \\ f'(\zeta) \to 0, \quad \theta(\zeta) \to 0, \quad as \quad \zeta \to \infty. \end{aligned}\right\} \tag{3.27}$$

Different parameters used in equations (3.25) and (3.26) are formulated as follows:

$$M^2 = \frac{\sigma B_0^2}{\rho a}, \qquad Pr = \frac{\mu C_p}{k}, \qquad B = \frac{Q}{a\rho C_p}.$$

The skin friction coefficient, is given as follows:

$$C_{fx} = \frac{\tau_w|_{y=0}}{\rho U_w^2(x)}. \tag{3.28}$$

To achive the dimensionless form of C_{fx} the following formula will be helpful:

$$\tau_w = \mu \left(\frac{\partial u}{\partial y}\right)_{y=0}. \tag{3.29}$$

As a result the dimensionless form of the skin friction coefficient gets the following form:

$$\begin{aligned} C_{fx} &= \frac{\mu \left(\frac{\partial u}{\partial y}\right)_{y=0}}{\rho U_w^2(x)}, \\ &= \frac{\mu \left(a\sqrt{\frac{a}{\nu}}x\right)}{\rho a^2 x^2} f''(0), \\ &= \frac{\rho\nu}{\rho a^{1/2} x} f''(0), \\ &= \frac{\sqrt{\nu}}{a^{1/2}} x f''(0), \\ &= \frac{1}{Re_x^{1/2}} f''(0), \\ \Rightarrow \quad Re_x^{1/2} C_{fx} &= f''(0), \end{aligned} \tag{3.30}$$

where Re_x denotes the Reynolds number defined as $Re_x = \frac{x u_w(x)}{\nu}$.

Local Nusselt number is defined as follows:

$$Nu_x = \frac{xq_w}{k(T - T_\infty)}. \tag{3.31}$$

To achive the dimensionless form of Nu_x the following formula will be helpful:

$$q_w = -k\left(\frac{\partial T}{\partial y}\right)_{y=0}. \tag{3.32}$$

As a result the dimensionless form of the Nusselt number gets the following form:

$$\begin{aligned} Nu_x &= \frac{-xk\left(\frac{\partial T}{\partial y}\right)_{y=0}}{k(T - T_\infty)}, \\ &= \frac{-x\frac{Dx^n}{k}\theta'(0)}{\frac{Dx^n}{k}\sqrt{\frac{\nu}{a}}}, \\ &= \frac{-xa^{1/2}}{\nu^{1/2}}\theta'(0), \\ &= -Re_x^{1/2}\theta'(0), \\ \Rightarrow \quad Re_x^{-1/2}Nu_x &= -\theta'(0). \end{aligned} \tag{3.33}$$

3.2 Numerical Method for Solution

The shooting method has been used to solve the ordinary differential equation (3.25). Use the notations given below for conversion of (3.25) to a system of first order ODEs:

$$f = y_1, \quad f' = y_1' = y_2, \quad f'' = y_1'' = y_2' = y_3, \quad f''' = y_3'.$$

Now the momentum equation (3.26) is converted into the following system of first order ODEs:

$$\begin{aligned} y_1' &= y_2, & y_1(0) &= S. \\ y_2' &= y_3, & y_2(0) &= \epsilon. \end{aligned}$$

$$y_3' = -y_1 y_3 + y_2^2 + M^2 y_2, \qquad y_3(0) = l.$$

"The above initial value problem will be numerically solved by RK-4 method. To get the approximate result, the domain of the problem has been taken as $[0, \zeta_\infty]$, where ζ_∞ is an approximate finite positive real number. The missing initial condition l for the above IVP satisfied the following equation."

$$(y_2(l))_{\zeta=\zeta_\infty} = 0.$$

For the convenience $(y_i(l))_{\zeta=\zeta_\infty}$ and the partial derivatives w.r.t l at $\zeta = \zeta_\infty$ will be denoted by $(y_i(l))$ and $\frac{\partial y_i}{\partial l}$ respectively.
Newton's method will be used to find l, which has the following iterative scheme:

$$l^{r+1} = l^r - \frac{y_2(l^r)}{\left(\frac{\partial}{\partial l}(y_2(l))\right)_{l=l^r}}, \quad r = 0, 1, 2....$$

With the help of the following notations, the above formula will be made to give the result.

$$\frac{\partial y_1}{\partial l} = y_4, \qquad \frac{\partial y_2}{\partial l} = y_5, \qquad \frac{\partial y_3}{\partial l} = y_6.$$

As a result of these new notations the Newton's iterative scheme gets the following form:

$$l^{r+1} = l^r - \frac{y_2(l^r)}{y_5(l^r)}.$$

Now differentiating the last system of three first order ODEs with respect to l, we get another system of three ODEs:

$$y_4' = y_5, \qquad y_4(0) = 0,$$
$$y_5' = y_6, \qquad y_5(0) = 0,$$

$$y_6' = -y_1 y_6 - y_3 y_4 + 2 y_2 y_5 + M^2 y_5, \qquad y_6(0) = 1.$$

The stoping criteria for the Newton's technique, is set as:

$$\mid y_2(l) \mid < \epsilon,$$

where $\epsilon > 0$ is an arbitrarily small positive number. From now onward, ϵ has been taken as 10^{-10}.

The equation (3.26) will be numerically solved by using shooting method by assuming f as a known function. For this, we utilize the following notions:

$$\theta = Z_1, \quad \theta' = Z_2, \quad \theta'' = Z_2'.$$

As a result, the energy equation (3.26) is converted into the following system of first order ODEs:

$$\begin{aligned} Z_1' &= Z_2, & Z_1(0) &= s. \\ Z_2' &= -PrfZ_2 + nPrf'Z_1 - PrBZ_1 & Z_2(0) &= -1. \end{aligned}$$

The above initial value problem IVP will be numerically solved by RK-4 technique.

The missing initial condition for the above IVP satisfy the following equation:

$$Z_1(s) = 0.$$

Now, we use Newton's method,

$$s^{r+1} = s^r - \frac{Z_1(s^r)}{\left(\frac{\partial}{\partial s}(Z_1(s))\right)_{s=s^r}}.$$

Next, introduce the following notations:

$$\frac{\partial Z_1}{\partial s} = Z_3, \qquad \frac{\partial Z_2}{\partial s} = Z_4.$$

As a result of these new notations, the Newton's iterative scheme get the following form:

$$s^{r+1} = s^r - \frac{Z_1(s^r)}{Z_3(s^r)}.$$

Now differentiate the above system of two first order ODEs with respect to s, to get two more first order ODEs:

$$\begin{aligned} Z_3' &= Z_4, & Z_3(0) &= 1, \\ Z_4' &= -PrfZ_4 + nPrf'Z_3 - PrBZ_3, & Z_4(0) &= 0. \end{aligned}$$

The above initial value problem will be numerically solved by RK-4 technique, to get the approximate solution.
The process will be repeated until the following stopping criteria is met:

$$|Z_1(s)| < \epsilon.$$

3.3 Analysis of Graphs and Tables

A thorough discussion on the graphs and tables has been conducted which contains the behaviour of different dimensionless parameters on the local skin friction coefficient $(Re_x)^{\frac{1}{2}}C_{fx}$ and local Nusselt number $(Re_x)^{-\frac{1}{2}}Nu_x$.
Table 3.1 explains the impact of suction parameter S, magnetic parameter M^2, stretching/shrinking parameter ϵ, on $(Re_x)^{\frac{1}{2}}C_{fx}$. For the rising values of S, the skin friction $(Re_x)^{\frac{1}{2}}C_{fx}$ increases. For increasing values of ϵ, the skin friction coefficient $(Re_x)^{\frac{1}{2}}C_{fx}$ is found to decrease. In this table, I_l is the interval from which the missing condition l can be chosen.
In Table 3.2, the effect of significant parameters like suction parameter S, magnetic parameter M^2, stretching/shrinking parameter ϵ, Prandtl number Pr and heat source parameter B on Nusselt number $(Re_x)^{-\frac{1}{2}}Nu_x$ has been discussed. The rising pattern is found in $(Re_x)^{-\frac{1}{2}}Nu_x$ due to increasing values of S. In this table,

I_s is the interval from which the missing condition s can be chosen.

Figure 3.2 reflects the behaviour of the temperature profile $\theta(\zeta)$ for different values of Pr without B. Pr is inversely related to thermal diffusivity, so by increasing values of Pr, the thermal diffusivity will be reduced. So if the value of Pr increases, the temperature profile will be decreased.

Figures 3.3 and 3.4 show the impact of the suction parameter S on the non-dimensional transverse velocity $f(\zeta)$ and longitudinal velocity profile $f'(\zeta)$. As the values of S increase, the velocities will also increase. The effect of porosity enhances the velocities. The effect of each value of S remains uniform as we move away from the wall.

Figure 3.5 reflects the impact of S on the temperature distribution $\theta(\zeta)$. By enhancing the suction parameter, the thermal boundary thickness will be decreased. A decrement will be observed in the temperature profile as the values of S increase.

Figures 3.6 and 3.7 reflect the impact of the magnetic field parameter M^2 on the transverse velocity $f(\zeta)$ and longitudinal velocity $f'(\zeta)$. As the values of M^2 increase, the dimensionless transverse and longitudinal velocities will also increase.

Figure 3.8 shows the impact of M^2 on the temperature distribution $\theta(\zeta)$. A decrement is observed in the temperature profile while we accelerate the values of M^2. It is due to reduction in thermal boundary layer thickness, so the temperature of the fluid will be decreased.

Figure 3.9 displays the impact of Pr on $\theta(\zeta)$. As the values of Pr increase, the temperature distribution will reduce its values. It is due the inverse relation between Pr and thermal diffusivity.

Figure 3.10 shows the influence of heat source parameter B on the temperature profile $\theta(\zeta)$. As we know that heat is directly related to temperature, if the values of B increase, so the temperature of fluid will also increase.

Figure 3.11 shows the impact of heat flux n on temperature distribution $\theta(\zeta)$. Heat flux is proportional to temperature difference between solid, liquid or gaseous media. So if the values of heat flux increase, the temperature of fluid will also increase.

Figure 3.12 shows the impact of stretching/shrinking parameter ϵ on the longitudinal velocity $f'(\zeta)$. It can be shown from the figure that the velocity profile is

enhanced for larger values of ϵ. This increase in the non-dimensional velocity of stretching is due to the greater value of ϵ and helps to cause more fluid deformation.

Figure 3.13 shows the influence of stretching/shrinking parameter ϵ on $\theta(\zeta)$. As the values of ϵ increase, the momentum boundary layer becomes thicker. Whereas with an increase in ϵ, a reduction will be observed in temperature distribution; leading to an increase in heat transfer.

TABLE 3.1: Results of $(Re_x)^{\frac{1}{2}}C_{fx}$ for various parameters

S	M^2	ϵ	$(Re_x)^{\frac{1}{2}}C_{fx}$	I_l
2.0	2.0	-1.0	2.414214	[0.1, 1.9]
3.0			3.302775	[0.4, 2.9]
4.0			4.236068	[0.1, 1.6]
5.0			5.192582	[-0.9,2.7]
6.0			6.162278	[-1.5,2.5]
7.0			7.162278	[-1.5,2.5]
8.0			8.162278	[-1.5,2.5]
3.0	0.0		2.618041	[1.0, 2.9]
	1.0		3.000000	[0.7, 2.3]
	2.0		3.302775	[0.4, 1.6]
	3.0		3.561552	[-0.1,1.8]
	4.0		3.791287	[-0.2,1.6]
	5.0		3.891287	[-0.3,1.6]
	6.0		3.991287	[-0.4,1.6]
	2.0		3.302775	[0.4, 0.9]
		-0.5	1.718246	[-0.8,0.5]
		0.5	-1.839725	[-1.9,1.5]
		1.0	-3.791287	[-2.0,0.9]
		1.5	-4.791287	[-2.0,0.9]
		2.0	-5.791287	[-2.0,0.9]

TABLE 3.2: Results of $-(Re_x)^{-\frac{1}{2}}Nu_x$ for various parameters

S	M^2	ϵ	Pr	B	n	$-(Re_x)^{-\frac{1}{2}}Nu_x$	I_s
2.0	2.0	-1.0	0.71	0.05	2.0	-1.332041	[0.6, 1.6]
3.0						-0.590706	[0.1, 2.9]
4.0						-0.397615	[0.3, 1.5]
5.0						-0.303852	[-0.5,2.5]
6.0						-0.247232	[-0.3,1.3]
3.0	0.0					-0.617806	[1.0, 3.9]
	1.0					-0.601214	[0.7, 2.3]
	2.0					-0.590706	[0.5, 2.2]
	3.0					-0.583077	[-0.1,0.8]
	4.0					-0.577130	[-0.3,0.9]
	2.0					-0.590706	[0.4, 1.2]
		-0.5				-0.522113	[-0.7,0.5]
		0.5				-0.436166	[-1.5,3.1]
		1.0				-0.406903	[-0.8,1.4]
		-1.0				-0.590706	[0.1, 3.8]
			1.00			-0.404932	[1.0, 4.0]
			1.50			-0.259153	[-0.1,1.6]
			2.30			-0.162535	[0.4, 1.8]
			7.00			-0.049831	[0.1, 1.9]
			0.71	0.00		-0.583253	[-0.8,0.1]
				0.05		-0.590706	[-0.7,0.5]
				0.08		-0.594951	[-0.2,0.1]
				0.10		-0.598013	[-0.3,0.2]
				0.30		-0.632231	[-0.4,0.9]
				0.05	-2.0	-0.445982	[-0.1,1.5]
					-1.0	-0.473579	[0.3, 0.9]
					0.0	-0.505873	[0.4, 1.2]
					1.0	-0.544200	[0.1, 2.2]
					2.0	-0.590706	[0.4, 0.9]

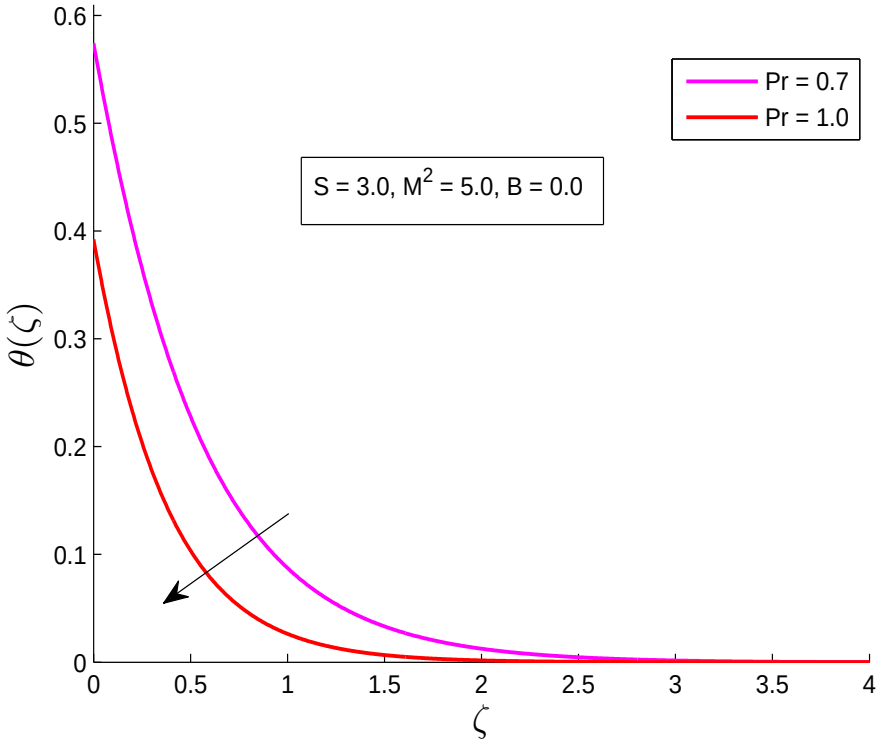

FIGURE 3.2: Impact of Pr on $\theta(\zeta)$ for $B = 0$.

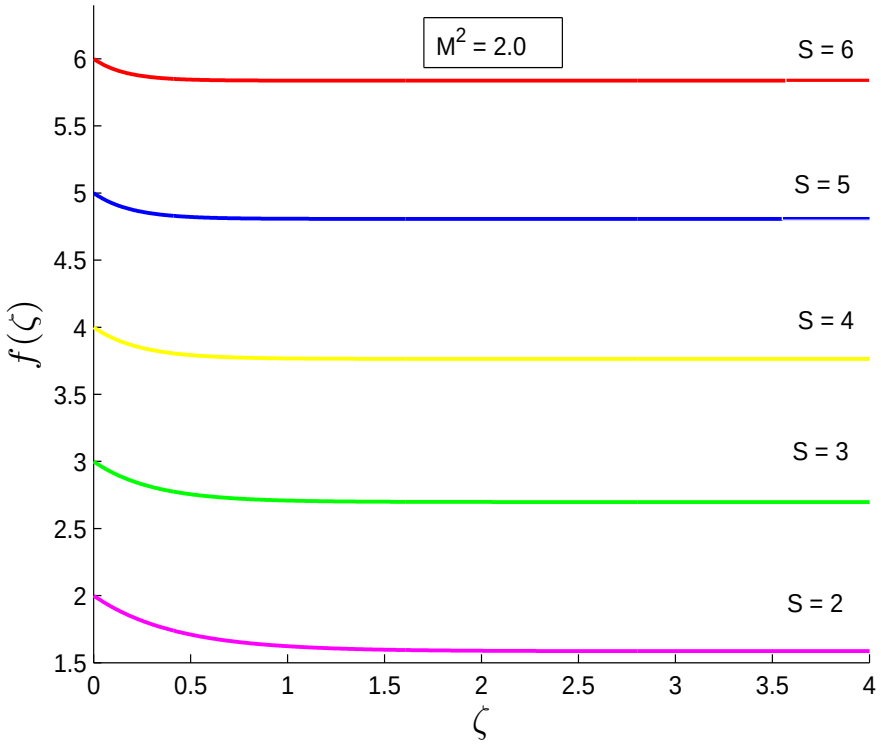

FIGURE 3.3: Impact of S on $f(\zeta)$ for $M^2 = 2$.

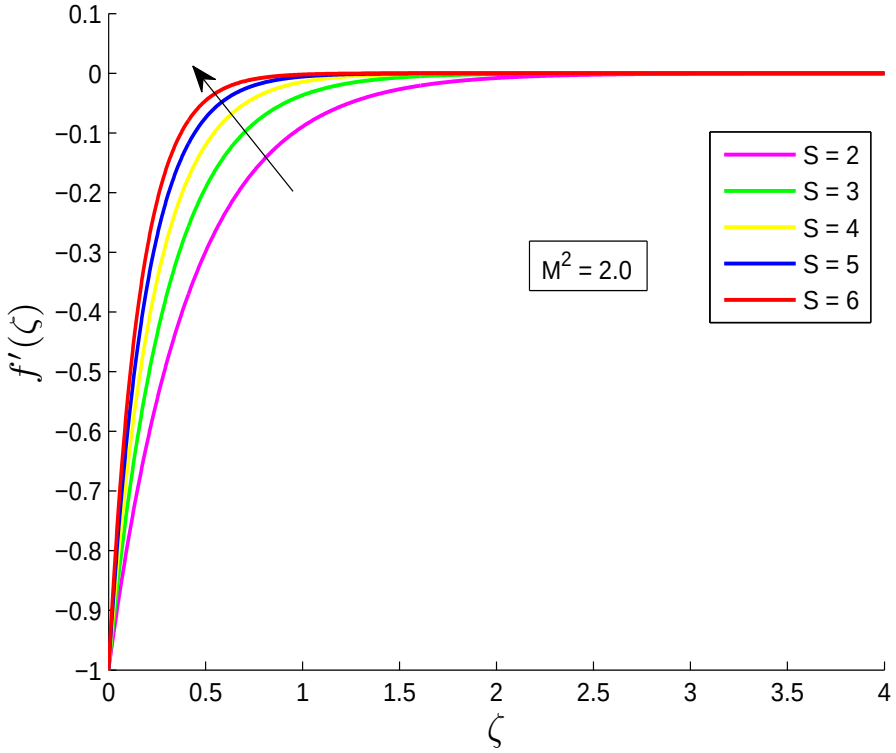

FIGURE 3.4: Impact of S on $f'(\zeta)$ for $M^2 = 2$.

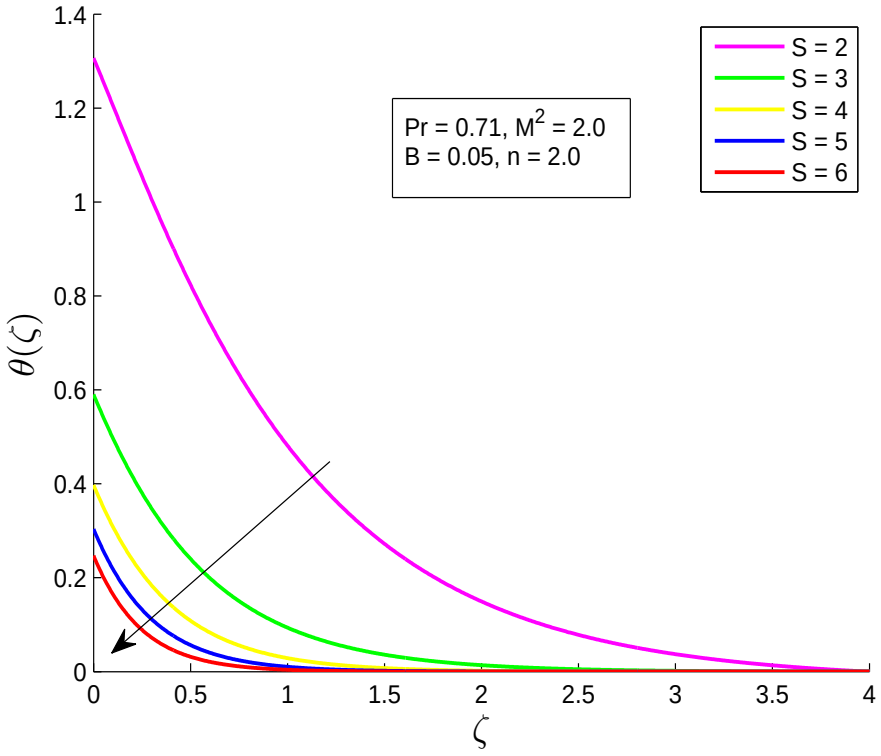

FIGURE 3.5: Influence of S on $\theta(\zeta)$ for $B = 0.05$.

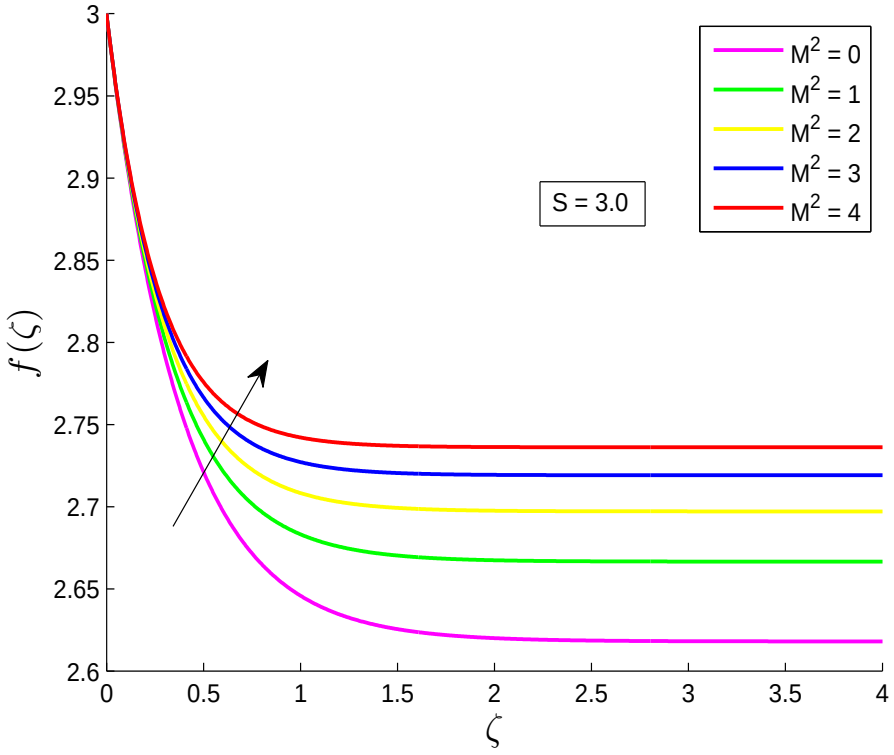

FIGURE 3.6: Impact of M^2 on transverse velocity profile.

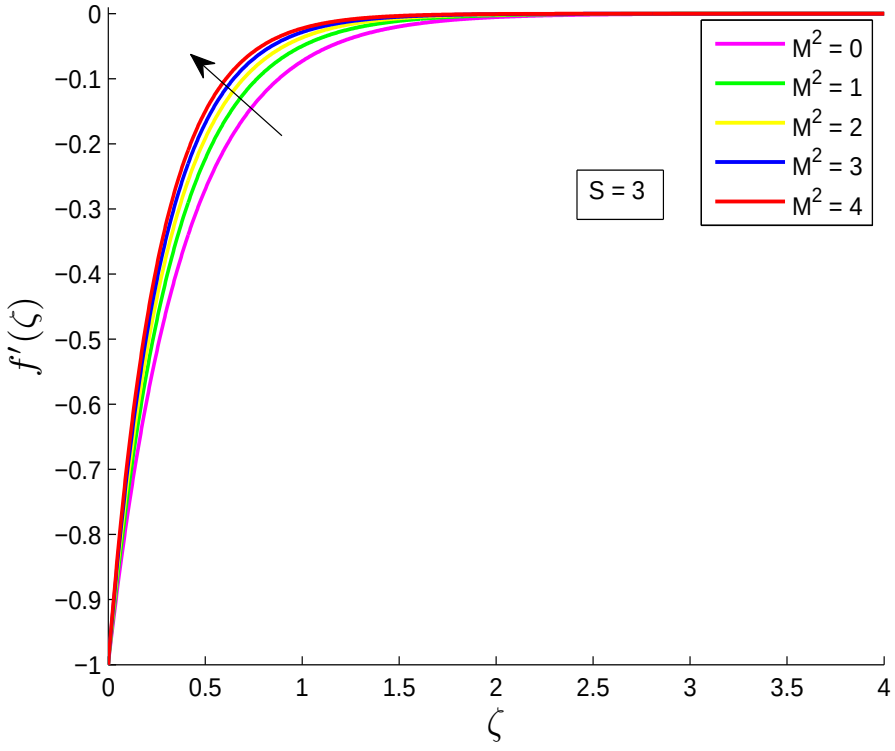

FIGURE 3.7: Impact of M^2 on dimensionless $f'(\zeta)$.

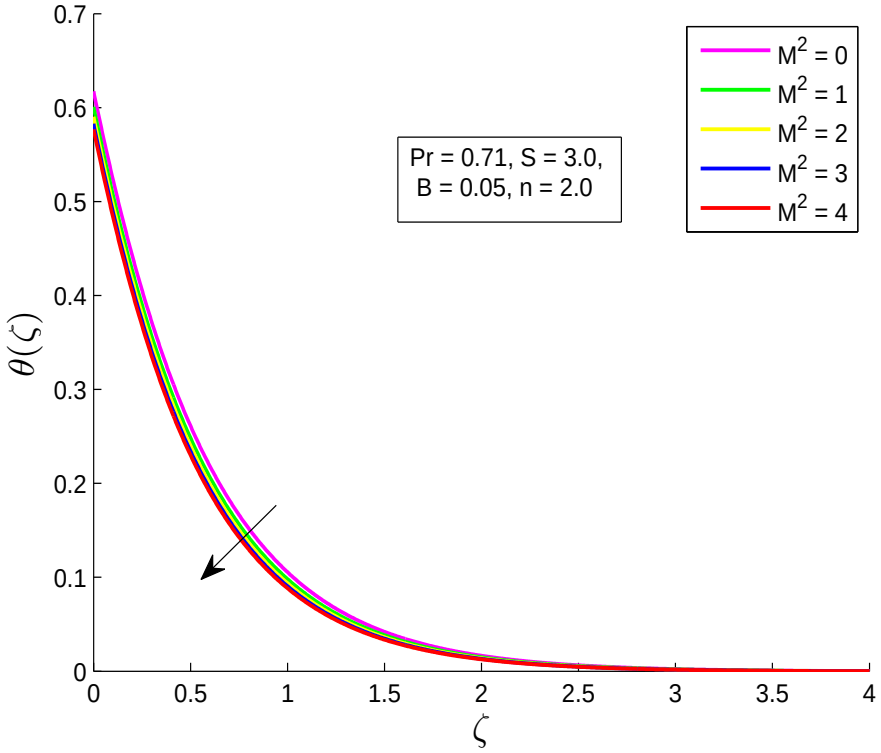

FIGURE 3.8: Influence of M^2 over temperature profile.

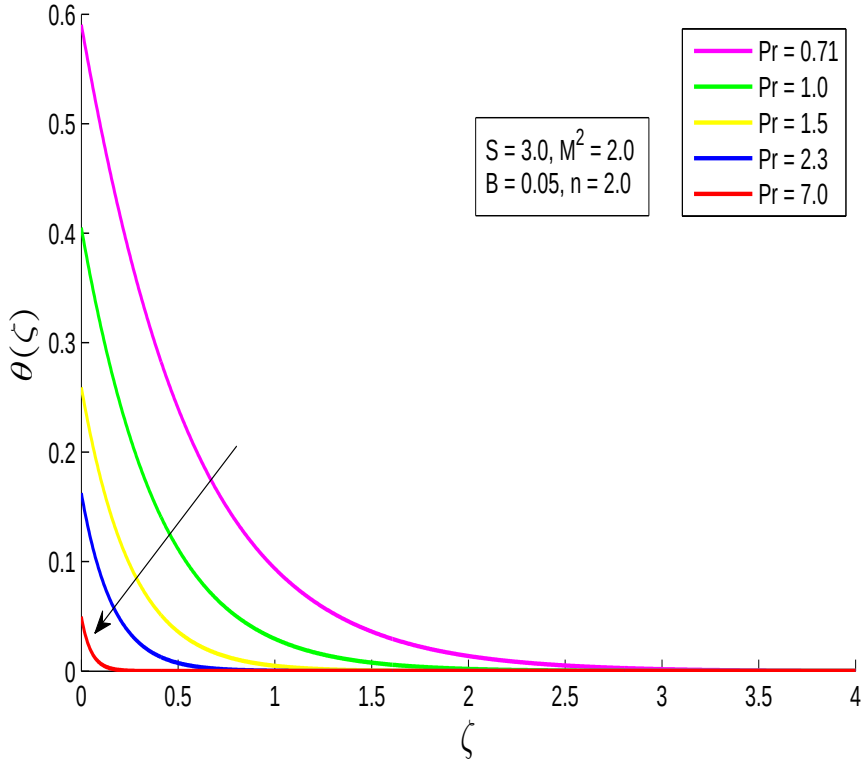

FIGURE 3.9: Effect of Pr over dimensionless temperature.

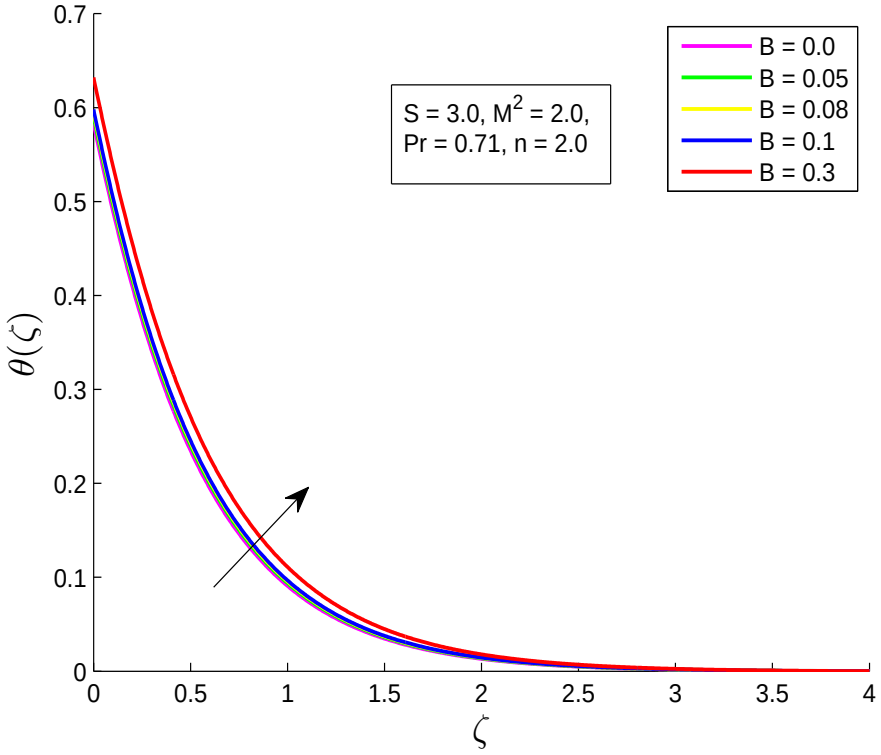

FIGURE 3.10: Impact of B on $\theta(\zeta)$.

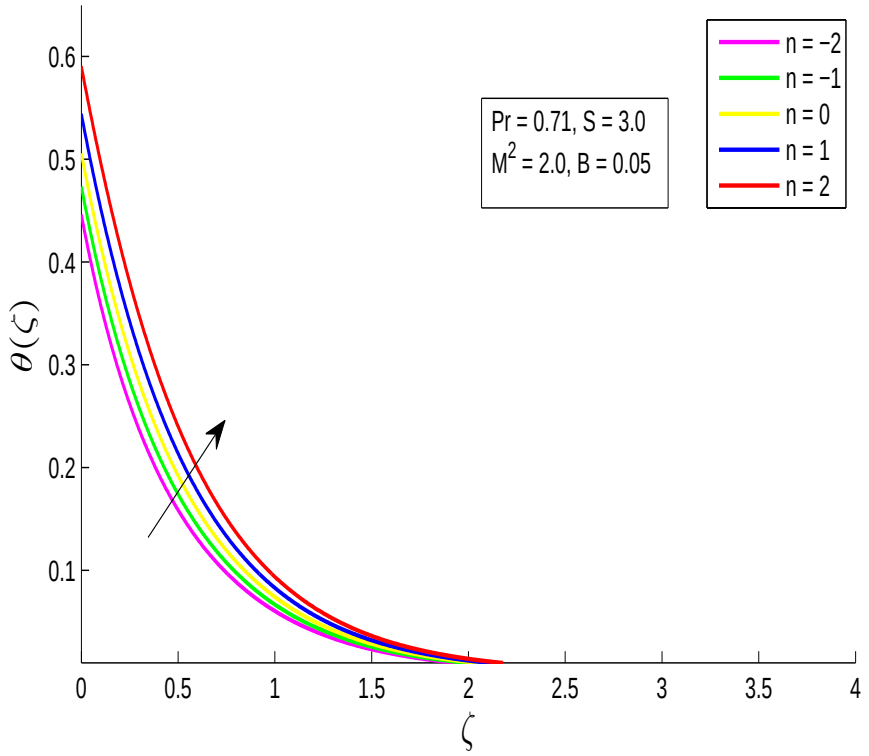

FIGURE 3.11: Impact of n on $\theta(\zeta)$.

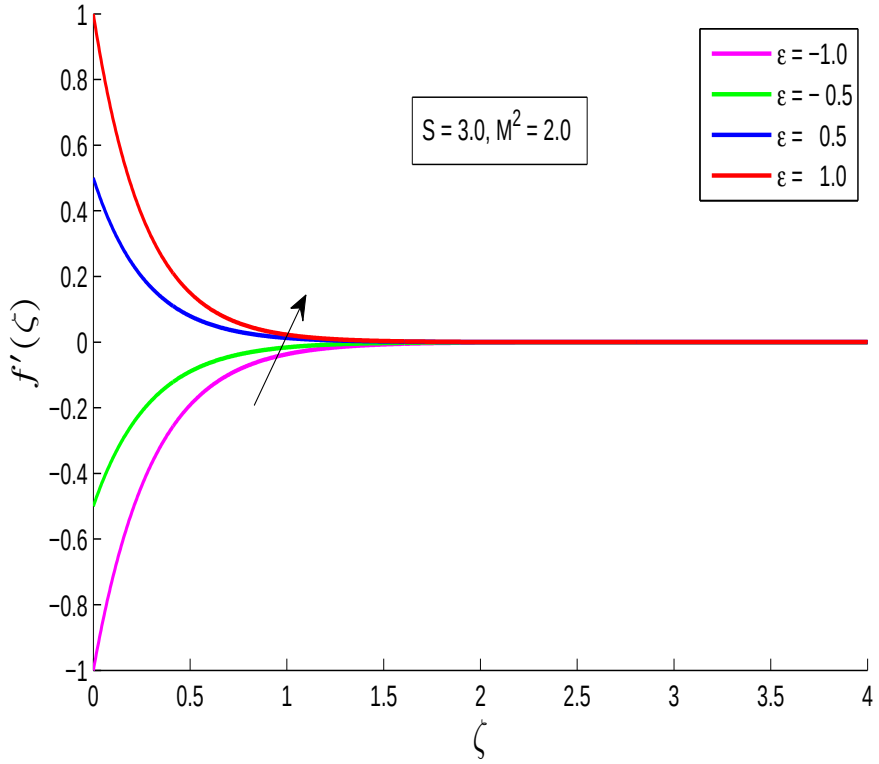

FIGURE 3.12: Impact of ϵ on longitudinal velocity profile.

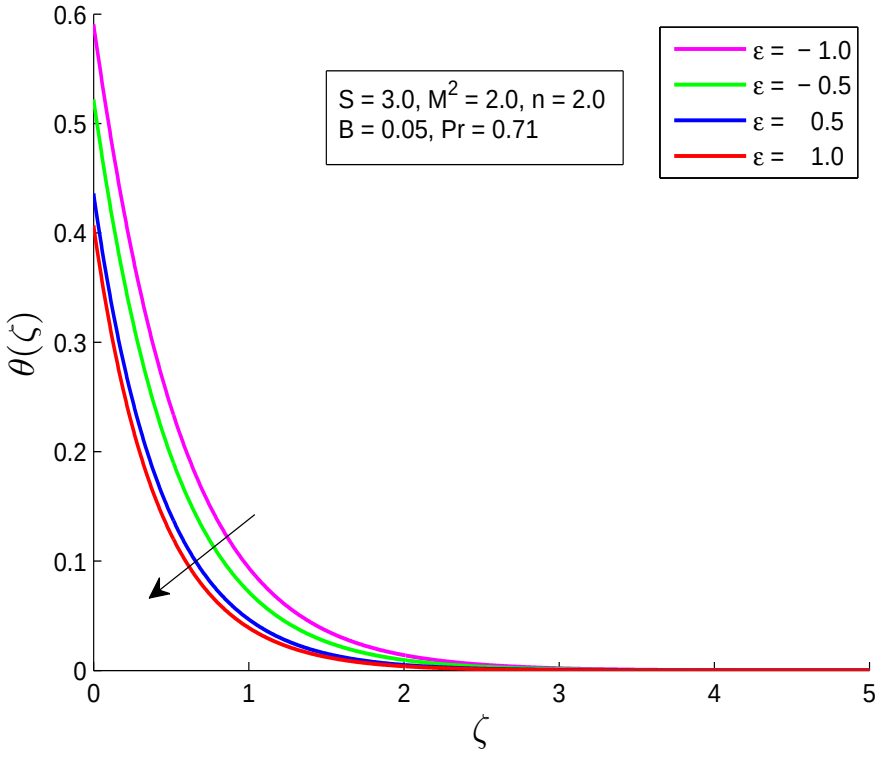

FIGURE 3.13: Influence of ϵ over temperature profile.

Chapter 4

Effect of Joule Heating and Arrhenius Activation Energy on MHD Boundary Layer Flow over a Stretching/Shrinking Sheet

4.1 Introduction

This chapter contains the extension of the model discussed in the last chapter. By considering additional impact of MHD, Joule heating , Thermophoresis diffusion and Brownian motion in temperature and concentration equation. We convert the concentration, temperature and momentum PDEs into set of ODEs by using the similarity transformation.

The familiar shooting technique has been used for the computation of the numerical solution of these ODEs. At the end of this chapter, the final results are discussed. Nusselt number and Sherwood number are shown in tables, while the impact of significant parameters on the temperature profile and concentration distribution are shown in graphs.

4.2 Mathematical Modeling

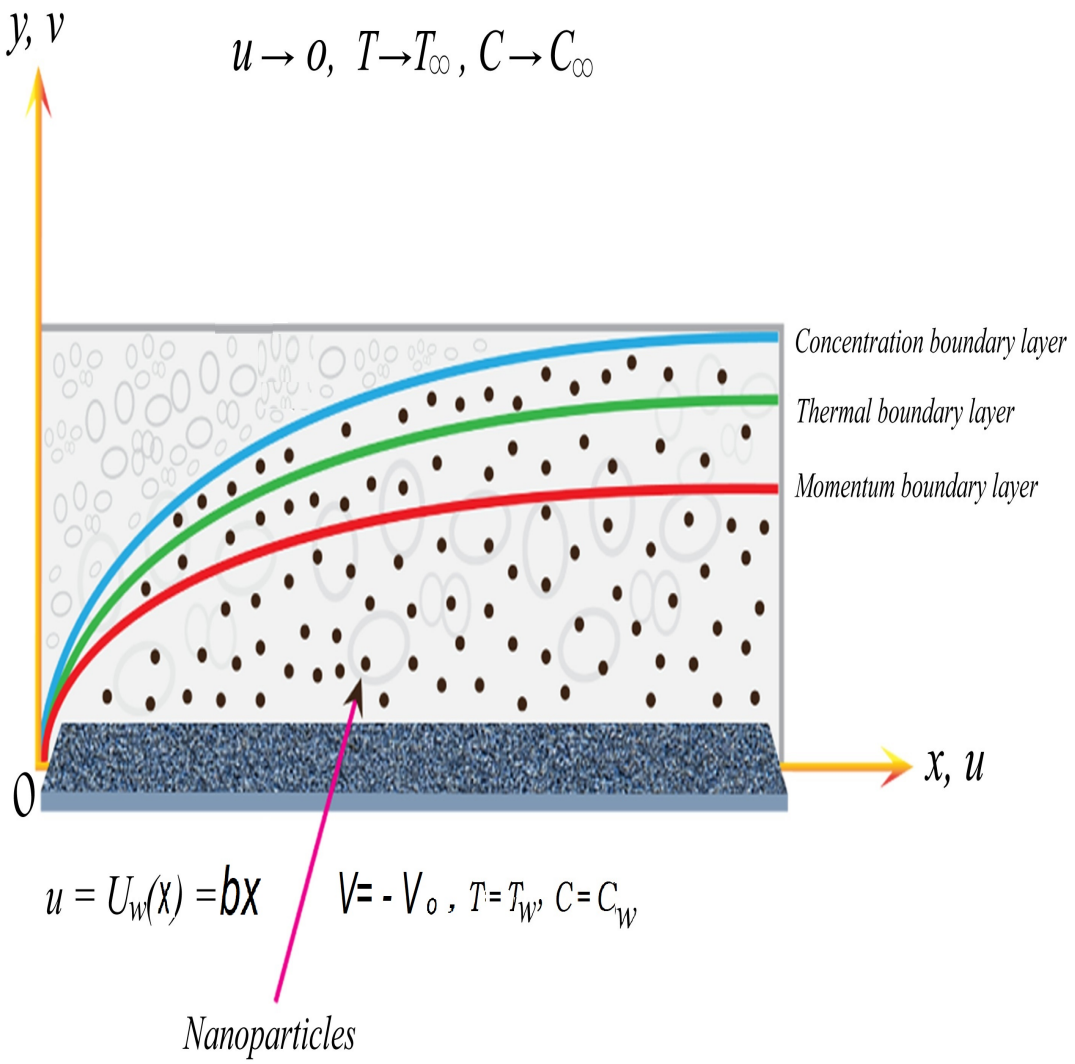

FIGURE 4.1: Systematic representation of physical model.

It is aimed to analyze a 2-D incompressible, steady and laminar MHD flow of viscous, electrically conducting fluid caused by a stretching/shrinking sheet in the presence of uniform magnetic field B_0. Furthermore, the direction of flow is taken along x-axis while y-axis normal to it. Energy transport analysis is aimed to be carried out in the presence of Joule heating, Brownian diffusion and thermophoresis diffusion. Moreover, the concentration of flow will be discussed with the help of concentration equation under the effect of activation energy and chemical reaction.

The system of equations describing the flow are given below:

$$\frac{\partial u}{\partial x}+\frac{\partial v}{\partial y}=0, \tag{4.1}$$

$$u\frac{\partial u}{\partial x}+v\frac{\partial u}{\partial y}=\nu\left(\frac{\partial^2 u}{\partial y^2}\right)-\frac{\sigma B_0^2}{\rho}u, \tag{4.2}$$

$$\begin{aligned}u\frac{\partial T}{\partial x}+v\frac{\partial T}{\partial y}&=\frac{k}{\rho C_p}\left(\frac{\partial^2 T}{\partial y^2}\right)+\frac{Q}{\rho C_p}(T-T_\infty)\\&\quad+\tau\left(D_B\frac{\partial C}{\partial y}\frac{\partial T}{\partial y}+\frac{D_T}{T_\infty}\left(\frac{\partial T}{\partial y}\right)^2\right)+\frac{\sigma B_0^2}{\rho C_p}u^2,\end{aligned} \tag{4.3}$$

$$\begin{aligned}u\frac{\partial C}{\partial x}+v\frac{\partial C}{\partial y}&=D_B\frac{\partial^2 C}{\partial y^2}+\left(\frac{D_T}{T_\infty}\right)\frac{\partial^2 T}{\partial y^2}\\&\quad-K_r^2\left(\frac{T}{T_\infty}\right)^m\exp\left[\frac{-E_a}{kT}\right](C-C_\infty).\end{aligned} \tag{4.4}$$

The associated BCs have been taken as:

$$\left.\begin{aligned}&u=U_w=bx,\quad v=-v_0,\quad T=T_w,\quad C=C_w\quad at\quad y=0.\\&u\to 0,\quad T\to T_\infty,\quad C\to C_\infty\quad as\quad y\to\infty.\end{aligned}\right\} \tag{4.5}$$

For the conversion of the mathematical model of PDEs (4.1)-(4.4) into the ODEs, the following similarity transformation have been considered:

$$\left.\begin{aligned}&\psi(x,y)=\sqrt{a\nu}f(\zeta),\\&\zeta=y\sqrt{\frac{a}{\nu}},\\&\theta(\zeta)=\frac{T-T_\infty}{T_w-T_\infty},\\&\phi(\zeta)=\frac{C-C_\infty}{C_w-C_\infty},\end{aligned}\right\} \tag{4.6}$$

where ψ denotes the stream function, ζ denotes the similarity variable, $\theta(\zeta)$ and $\phi(\zeta)$ are the dimensionless temperature and concentration.

The detailed procedure for the conversion of (4.1) and (4.2) into the dimensionaless form has been already discussed in chapter 3.

Now, included below is the procedure for the conversion of (4.3) into the dimensionless form:

- $$\frac{\partial T}{\partial x} = (T_w - T_\infty)\theta'(\zeta)\frac{\partial \zeta}{\partial x}$$
$$= 0. \tag{4.7}$$
- $$\frac{\partial T}{\partial y} = (T_w - T_\infty)\,\theta'(\zeta)\frac{\partial \zeta}{\partial y}$$
$$= (T_w - T_\infty)\sqrt{\frac{a}{\nu}}\theta'(\zeta). \tag{4.8}$$
- $$\frac{\partial^2 T}{\partial y^2} = (T_w - T_\infty)\left(\frac{a}{\nu}\right)\theta''(\zeta). \tag{4.9}$$
- $$\frac{\partial C}{\partial x} = (C_w - C_\infty)\phi'(\zeta)\frac{\partial \zeta}{\partial x}$$
$$= 0. \tag{4.10}$$
- $$\frac{\partial C}{\partial y} = (C_w - C_\infty)\phi'(\zeta)\frac{\partial \zeta}{\partial y}$$
$$= (C_w - C_\infty)\sqrt{\frac{a}{\nu}}\phi'(\zeta). \tag{4.11}$$
- $$\frac{\partial^2 C}{\partial y^2} = (C_w - C_\infty)\frac{a}{\nu}\phi''(\zeta). \tag{4.12}$$
- $$u\frac{\partial T}{\partial x} = 0. \tag{4.13}$$
- $$v\frac{\partial T}{\partial y} = -\sqrt{a\nu}f(\zeta)(T_w - T_\infty)\sqrt{\frac{a}{\nu}}\theta'(\zeta)$$
$$= -a(T_w - T_\infty)f(\zeta)\theta'(\zeta). \tag{4.14}$$
- $$\frac{k}{\rho Cp}\frac{\partial^2 T}{\partial y^2} = \frac{k}{\rho Cp}(T_w - T_\infty)\left(\frac{a}{\nu}\right)\theta''(\zeta). \tag{4.15}$$
- $$\frac{Q}{\rho Cp}(T - T_\infty) = \frac{Q}{\rho Cp}(T_w - T_\infty)\theta(\zeta). \tag{4.16}$$
- $$\tau D_B\frac{\partial C}{\partial y}\frac{\partial T}{\partial y} = \tau D_B\frac{a}{\nu}(C_w - C_\infty)(T_w - T_\infty)\theta'(\zeta)\phi'(\zeta). \tag{4.17}$$
- $$\tau\frac{D_T}{T_\infty}\left(\frac{\partial T}{\partial y}\right)^2 = \tau\frac{D_T}{T_\infty}\left[(T_w - T_\infty)\sqrt{\frac{a}{\nu}}\theta'(\zeta)\right]^2$$
$$= \tau\frac{D_T}{T_\infty}\frac{a}{\nu}(T_w - T_\infty)^2\theta'^2(\zeta). \tag{4.18}$$
- $$\frac{\sigma}{\rho Cp}B_0^2u^2 = \frac{\sigma}{\rho Cp}B_0^2a^2x^2f'^2(\zeta). \tag{4.19}$$

Using (4.13) and (4.14), in the left side of (4.3), we get the following:

$$u\frac{\partial T}{\partial x}+v\frac{\partial T}{\partial y}=-a(T_w-T_\infty)f(\zeta)\theta'(\zeta). \tag{4.20}$$

Using (4.15) to (4.19) in the right side of (4.3), we get the following:

$$\begin{aligned}
&\frac{k}{\rho C_p}\left(\frac{\partial^2 T}{\partial y^2}\right)+\frac{Q}{\rho C_p}(T-T_\infty)+\tau\left(D_B\frac{\partial C}{\partial y}\frac{\partial T}{\partial y}+\frac{D_T}{T_\infty}\left(\frac{\partial T}{\partial y}\right)^2\right)+\frac{\sigma B_0^2}{\rho C_p}u^2\\
&=\frac{k}{\rho Cp}(T_w-T_\infty)\left(\frac{a}{\nu}\right)\theta''(\zeta)+\frac{Q}{\rho Cp}(T_w-T_\infty)\theta(\zeta)+\frac{\sigma}{\rho Cp}B_0^2a^2x^2f'^2(\zeta)\\
&\quad+\tau D_B\frac{a}{\nu}(C_w-C_\infty)(T_w-T_\infty)\theta'(\zeta)\phi'(\zeta)+\tau\frac{D_T}{T_\infty}\frac{a}{\nu}(T_w-T_\infty)^2\theta'^2(\zeta)\\
&=a(T_w-T_\infty)[\frac{k}{\rho Cp\nu}\theta''(\zeta)+\frac{Q}{a\rho Cp}\theta(\zeta)+\frac{\tau D_B}{\nu}(C_w-C_\infty)\theta'(\zeta)\phi'(\zeta)\\
&\quad+\frac{\tau D_T}{T_\infty\nu}(T_w-T_\infty)\theta'^2(\zeta)+\frac{\sigma}{\rho Cp(T_w-T_\infty)}B_0^2ax^2f'^2(\zeta)]\\
&=a\left(T_w-T_\infty\right)\left[\frac{1}{Pr}\theta''(\zeta)+B\theta(\zeta)+Nb\theta'(\zeta)\phi'(\zeta)+Nt\theta'^2(\zeta)+M^2Ecf'^2(\zeta)\right].
\end{aligned} \tag{4.21}$$

With the help of (4.20) and (4.21), the following dimensionless form of (4.3) is obtained:

$$\begin{aligned}
&-f(\zeta)\theta'(\zeta)=\frac{1}{Pr}\theta''(\zeta)+B\theta(\zeta)+Nb\theta'(\zeta)\phi'(\zeta)+N_t\theta'^2(\zeta)+M^2Ecf'^2(\zeta).\\
\Rightarrow\ &\frac{1}{Pr}\theta''(\zeta)+B\theta(\zeta)+f(\eta)\theta'(\zeta)+Nb\theta'(\zeta)\phi'(\zeta)+N_t\theta'^2(\zeta)+M^2Ecf'^2(\zeta)=0.
\end{aligned} \tag{4.22}$$

Now, the conversion involved to get (4.4) converted into the dimensionless form are:

- $$\begin{aligned}
D_B\frac{\partial^2 C}{\partial y^2}&=D_B\frac{a}{\nu}\left(C_w-C_\infty\right)\phi''(\zeta)\\
&=a\left(C_w-C_\infty\right)\left[\frac{D_B}{\nu}\phi''(\zeta)\right]\\
&=a\left(C_w-C_\infty\right)\left[\frac{1}{Sc}\phi''(\zeta)\right].
\end{aligned} \tag{4.23}$$

- $$\frac{D_T}{T_\infty}\frac{\partial^2 T}{\partial y^2} = \frac{D_T}{T_\infty}\frac{a}{\nu}\left(T_w - T_\infty\right)\theta''(\zeta)$$
$$= a\left(C_w - C_\infty\right)\left[\frac{D_T}{T_\infty \nu}\left(\frac{T_w - T_\infty}{C_w - C_\infty}\right)\theta''(\zeta)\right]$$
$$= a\left(C_w - C_\infty\right)\frac{D_B}{\nu}\left[\frac{D_T}{T_\infty D_B}\left(\frac{T_w - T_\infty}{C_w - C_\infty}\right)\theta''(\zeta)\right]$$
$$= a\left(C_w - C_\infty\right)\frac{1}{Sc}\frac{N_t}{N_b}\theta''(\zeta). \tag{4.24}$$
- $$k_r^2\left(\frac{T}{T_\infty}\right)^m exp\left[-\frac{E_a}{kT}\right]\left(C_w - C_\infty\right)$$
$$= k_r^2\left(1 + \left(\frac{T_w - T_\infty}{T_\infty}\right)\theta(\zeta)\right)^m exp\left(\frac{-\frac{E_a}{kT_\infty}}{1 + \left(\frac{T_w - T_\infty}{T_\infty}\right)\theta(\zeta)}\right)\left(C_w - C_\infty\right)\phi(\zeta)$$
$$= a\left(C_w - C_\infty\right)\left[\sigma^*\left(1 + \delta\theta(\zeta)\right)^m exp\left(\frac{-E_1}{1 + \delta\theta(\zeta)}\right)\phi(\zeta)\right]. \tag{4.25}$$

Now use (4.10) and (4.11) to convert the left hand side of (4.4) into the dimensionless form. The left hand side of (4.4), get the form:

$$u\frac{\partial C}{\partial x} + v\frac{\partial C}{\partial y} = axf'(\zeta)\left[0\right] + \left[-\sqrt{a\nu}f(\zeta)\right]\left(C_w - C_\infty\right)\sqrt{\frac{a}{\nu}}\phi'(\zeta)$$
$$= -a\left(C_w - C_\infty\right)f(\zeta)\phi'(\zeta). \tag{4.26}$$

Now by using (4.23), (4.24) and (4.25) in the right hand side of (4.4), we get:

$$D_B\frac{\partial^2 C}{\partial y^2} + \left(\frac{D_T}{T_\infty}\right)\frac{\partial^2 T}{\partial y^2} - K_r^2\left(\frac{T}{T_\infty}\right)^m \exp\left[\frac{-E_a}{kT}\right]\left(C - C_\infty\right).$$

$$= a\left(C_w - C_\infty\right)\left[\frac{1}{Sc}\phi''(\zeta) + \frac{1}{Sc}\frac{N_t}{N_b}\theta''(\zeta) - \sigma^*\left(1 + \delta\theta(\zeta)\right)^m exp\left(\frac{-E_1}{1 + \delta\theta(\zeta)}\right)\phi(\zeta)\right]. \tag{4.27}$$

From (4.26) and (4.27), the dimensionless form of (4.4) is:

$$-f(\zeta)\phi'(\zeta) = \frac{1}{Sc}\phi''(\zeta) + \frac{1}{Sc}\frac{N_t}{N_b}\theta''(\zeta) - \sigma^*\left(1 + \delta\theta(\zeta)\right)^m exp\left(\frac{-E_1}{1 + \delta\theta(\zeta)}\right)\phi(\zeta)$$
$$\Rightarrow \frac{1}{Sc}\phi''(\zeta) + \frac{1}{Sc}\frac{N_t}{N_b}\theta''(\zeta) - \sigma^*\left(1 + \delta\theta(\zeta)\right)^m exp\left(\frac{-E_1}{1 + \delta\theta(\zeta)}\right)\phi(\zeta) + f(\zeta)\phi'(\zeta) = 0. \tag{4.28}$$

The associated boundary conditions will be converted through the following procedure:

$$
\begin{aligned}
\bullet \quad & u = U_w(x) = bx, && at \quad y = 0.\\
\Rightarrow \quad & u = axf'(\zeta), && at \quad \zeta = 0.\\
\Rightarrow \quad & af'(\zeta)x = bx, && at \quad \zeta = 0.\\
\Rightarrow \quad & f'(\zeta) = \epsilon, \qquad \epsilon = b/a, && at \quad \zeta = 0.\\
\Rightarrow \quad & f'(\zeta) = \epsilon, && at \quad \zeta = 0.\\
\bullet \quad & v = -v_0, && at \quad y = 0.\\
\Rightarrow \quad & v = -\sqrt{a\nu} f(\zeta), && at \quad \zeta = 0.\\
\Rightarrow \quad & -\sqrt{a\nu} f(\zeta) = -v_0, && at \quad \zeta = 0.\\
\Rightarrow \quad & f(\zeta) = \frac{v_0}{\sqrt{a\nu}}, && at \quad \zeta = 0.\\
\Rightarrow \quad & f(\zeta) = S, && at \quad \zeta = 0.\\
\bullet \quad & -\frac{\partial T}{\partial y} = -\sqrt{\frac{a}{\nu}}\,(T_w - T_\infty)\,, && at \quad y = 0.\\
\Rightarrow \quad & \frac{\partial T}{\partial y} = (T_w - T_\infty)\sqrt{\frac{a}{\nu}}\theta'(\zeta), && at \quad \zeta = 0.\\
\Rightarrow \quad & -\sqrt{\frac{a}{\nu}}\,(T_w - T_\infty) = (T_w - T_\infty)\sqrt{\frac{a}{\nu}}\theta'(\zeta), && at \quad \zeta = 0.\\
\Rightarrow \quad & \theta'(\zeta) = -1, && at \quad \zeta = 0.\\
\bullet \quad & C = C_w, && at \quad y = 0.\\
\Rightarrow \quad & \phi(\zeta)\,(C_w - C_\infty) + C_\infty = C_w, && at \quad \zeta = 0.\\
\Rightarrow \quad & \phi(\zeta)\,(C_w - C_\infty) = C_w - C_\infty, && at \quad \zeta = 0.\\
\Rightarrow \quad & \phi(\zeta) = 1, && at \quad \zeta = 0.\\
\bullet \quad & u \to (0), && as \quad y \to \infty.\\
\Rightarrow \quad & af'(\zeta)x \to (0), && as \quad \zeta \to \infty.\\
\Rightarrow \quad & f'(\zeta) \to (0), && as \quad \zeta \to \infty.\\
\bullet \quad & T \to T_\infty, && as \quad y \to \infty.\\
\Rightarrow \quad & \theta(\zeta)(T_w - T_\infty) + T_\infty \to T_\infty, && as \quad \zeta \to \infty.\\
\Rightarrow \quad & \theta(\zeta)(T_w - T_\infty) \to 0, && as \quad \zeta \to \infty.\\
\Rightarrow \quad & \theta(\zeta) \to 0, && as \quad \zeta \to \infty.
\end{aligned}
$$

$$
\begin{aligned}
\bullet \quad & C \to C_\infty, && as \quad y \to \infty. \\
\Rightarrow \quad & \phi(\zeta)\,(C_w - C_\infty) + C_\infty \to C_\infty, && as \quad \zeta \to \infty. \\
\Rightarrow \quad & \phi(\zeta)\,(C_w - C_\infty) + C_\infty \to 0, && as \quad \zeta \to \infty. \\
\Rightarrow \quad & \phi(\zeta) \to 0, && as \quad \zeta \to \infty.
\end{aligned}
$$

The final dimensionless form of the governing model is:

$$\frac{1}{Pr}\theta''(\zeta) + B\theta(\zeta) + f(\zeta)\theta'(\zeta) + Nb\theta'(\zeta)\phi'(\zeta) + N_t\theta'^2(\zeta) + M^2 Ecf'^2(\zeta) = 0. \tag{4.29}$$

$$\frac{1}{Sc}\phi''(\zeta) + \frac{1}{Sc}\frac{N_t}{N_b}\theta''(\zeta) - \sigma\,(1+\delta\theta(\zeta))^m\, exp\left[\frac{-E_1}{1+\delta\theta(\zeta)}\right]\phi(\zeta) + f(\zeta)\phi'(\zeta) = 0. \tag{4.30}$$

The associated BCs (4.5) in the dimensionless form are as follow:

$$\left.\begin{aligned} &\theta'(0) = -1, \quad \phi(0) = 1 \\ &\theta(\zeta) \to 0, \quad \phi(\zeta) \to 0, \quad as \quad \zeta \to \infty. \end{aligned}\right\} \tag{4.31}$$

Different parameters used in equations (4.29) and (4.30) are formulated as follows:

$$
\begin{aligned}
&M^2 = \frac{\sigma B_0^2}{\rho a}, \quad Pr = \frac{\mu C_p}{k}, \quad B = \frac{Q}{a\rho C_p}, \quad Ec = \frac{a^2x^2}{Cp(T_w - T_\infty)}, \\
&Nb = \frac{\tau D_B(C_w - C_\infty)}{\nu_f}, \quad Nt = \frac{\tau D_T(T_w - T_\infty)}{T_\infty \nu_f}, \quad Sc = \frac{\nu}{D_B}, \\
&\sigma^* = \frac{k_r^2}{a}, \quad \delta = \frac{T_w - T_\infty}{T_\infty}, \quad E_1 = \frac{E_a}{kT_\infty}.
\end{aligned}
$$

The local Nusselt number is defined as follows:

$$Nu_x = \frac{xq_w}{k(T_w - T_\infty)}. \tag{4.32}$$

To achive the dimensionless form of Nu_x, the following formula will be helpful.

$$q_w = -k\left(\frac{\partial T}{\partial y}\right)_{y=0}. \tag{4.33}$$

As a result,

$$\begin{aligned} Nu_x &= -\frac{kx}{k(T_w - T_\infty)} \left(\frac{\partial T}{\partial y}\right)_{y=0} \\ &= -\frac{x}{(T_w - T_\infty)}(T_w - T_\infty)\sqrt{\frac{a}{\nu}}\theta'(0) \\ &= -\sqrt{\frac{x^2 a}{\nu}}\theta'(0) \\ &= -(Re_x)^{\frac{1}{2}}\theta'(0) \\ \Rightarrow \qquad (Re_x)^{-\frac{1}{2}} Nu_x &= -\theta'(0), \end{aligned} \tag{4.34}$$

where

$$, \qquad Re_x = \frac{x u_w(x)}{\nu}.$$

The local Sherwood number are defined as:

$$Sh_x = \frac{x q_m}{D_B(C_w - C_\infty)}. \tag{4.35}$$

To achive the dimensionless form of of Sh_x, the following formula will be helpful.

$$q_w = -D_B \left(\frac{\partial C}{\partial y}\right)_{y=0} \tag{4.36}$$

As a result,

$$\begin{aligned} Sh_x &= -\frac{x D_B}{D_B(C_w - C_\infty)} \left(\frac{\partial C}{\partial y}\right)_{y=0} \\ &= -\frac{x}{C_w - C_\infty}\sqrt{\frac{a}{\nu}}\,(C_w - C_\infty)\,\phi'(0) \\ &= -x\sqrt{\frac{a}{\nu}}\phi'(0) \\ &= -\sqrt{\frac{a x^2}{\nu}}\phi'(0) \\ &= -(Re_x)^{\frac{1}{2}}\phi'(0) \\ (Re_x)^{-\frac{1}{2}} Sh_x &= -\phi'(0). \end{aligned} \tag{4.37}$$

4.3 Numerical Method for Solution

The shooting method has been used to solved ODEs (4.29) and (4.30). The following notations have been considered:

$$\theta = Y_1, \quad \theta' = Y_1' = Y_2, \quad \theta'' = Y_1'' = Y_2',$$
$$\phi = Y_3, \quad \phi' = Y_3' = Y_4, \quad \phi'' = Y_4'.$$

By using the notations, the following system of first order ODEs is obtained:

$$\begin{aligned}
Y_1' &= Y_2, && Y_1(0) = p,\\
Y_2' &= -Pr\left(BY_1 + fY_2 + NbY_2Y_4 + NtY_2^2 + M^2Ecf'^2\right), && Y_2(0) = -1,\\
Y_3' &= Y_4, && Y_3(0) = 1,\\
Y_4' &= -ScfY_4 + \frac{Nt}{Nb}Pr\left(BY_1 + fY_2 + NbY_2Y_4 + NtY_2^2 + M^2Ecf'^2\right)\\
&\quad + Sc\sigma^*\left(1+\delta Y_1\right)^m \exp\left[\frac{-E_1}{1+\delta Y_1}\right] Y_3, && Y_4(0) = q.
\end{aligned}$$

The above IVP will be numerically solved by RK-4 technique. For the approximate result, the domain of the problem has been chosen from $[0, \zeta_\infty]$, where ζ_∞ is an approximate finite positive real number. The missing initial conditions for the above IVP satisfy the following equation.

$$(Y_1(p,q))_{\zeta=\zeta_\infty} = 0, \qquad (Y_3(p,q))_{\zeta=\zeta_\infty} = 0.$$

For convenience $(Y_i(p,q))_{\zeta=\zeta_\infty}$ and their partial derivatives w.r.t p and q will be denoted by $(Y_i(p,q))$, $\frac{\partial Y_i}{\partial p}$ and $\frac{\partial Y_i}{\partial q}$.
To solve the above algebraic equations, we apply the Newton's method which has the following scheme:

$$\begin{bmatrix} p^{r+1} \\ q^{r+1} \end{bmatrix} = \begin{bmatrix} p^r \\ q^r \end{bmatrix} - \left(\begin{bmatrix} \frac{\partial Y_1}{\partial p} & \frac{\partial Y_1}{\partial q} \\ \frac{\partial Y_1}{\partial p} & \frac{\partial Y_3}{\partial q} \end{bmatrix}^{-1} \begin{bmatrix} Y_1 \\ Y_3 \end{bmatrix} \right)_{(p^r, q^r)}$$

Now, introduce the following notations:

$$\frac{\partial Y_1}{\partial p} = Y_5, \quad \frac{\partial Y_2}{\partial p} = Y_6, \quad \frac{\partial Y_3}{\partial p} = Y_7, \quad \frac{\partial Y_4}{\partial p} = Y_8.$$
$$\frac{\partial Y_1}{\partial q} = Y_9, \quad \frac{\partial Y_2}{\partial q} = Y_{10}, \quad \frac{\partial Y_3}{\partial q} = Y_{11}, \quad \frac{\partial Y_4}{\partial q} = Y_{12}.$$

As a result of these new notations, the Newton's iterative scheme gets the form:

$$\begin{bmatrix} p^{r+1} \\ q^{r+1} \end{bmatrix} = \begin{bmatrix} p^r \\ q^r \end{bmatrix} - \left(\begin{bmatrix} Y_5 & Y_9 \\ Y_7 & Y_{11} \end{bmatrix}^{-1} \begin{bmatrix} Y_1 \\ Y_3 \end{bmatrix} \right)_{(p^r, q^r)}$$

Now differentiate the last system of four first order ODEs with respect to p and q to get the following system of first order eight ODEs:

$$Y_5' = Y_6, \qquad Y_5(0) = 1,$$
$$Y_6' = -Pr\left(BY_5 + fY_6 + Nb\left(Y_2Y_8 + Y_6Y_4\right) + 2NtY_2Y_6\right), \qquad Y_6(0) = 0,$$
$$Y_7' = Y_8, \qquad Y_7(0) = 0,$$
$$\begin{aligned} Y_8' = {} & -ScfY_8 + \frac{Nt}{Nb} Pr\left(BY_5 + fY_6 + Nb\left(Y_2Y_8 + Y_6Y_4\right) + 2NtY_2Y_6\right) \\ & + \sigma^* Sc\left(1 + \delta Y_1\right)^m \exp\left[\frac{-E_1}{1 + \delta Y_1}\right] Y_7 \\ & + Sc\left(1 + \delta Y_1\right)^{m-2} \exp\left[\frac{-E_1}{1 + \delta Y_1}\right] E_1 \delta \sigma^* Y_5 Y_3 \\ & + Sc\, m\left(1 + \delta Y_1\right)^{m-1} \exp\left[\frac{-E_1}{1 + \delta Y_1}\right] \delta \sigma^* Y_5 Y_3, \qquad Y_8(0) = 0. \end{aligned}$$
$$Y_9' = Y_{10}, \qquad Y_9(0) = 0.$$
$$Y_{10}' = -Pr\left(BY_9 + fY_{10} + Nb\left(Y_2Y_{12} + Y_{10}Y_4\right) + 2NtY_2Y_{10}\right), \qquad Y_{10}(0) = 0.$$
$$Y_{11}' = Y_{12}, \qquad Y_{11}(0) = 0.$$
$$\begin{aligned} Y_{12}' = {} & -ScfY_{12} + \frac{Nt}{Nb} Pr\left(BY_9 + fY_{10} + Nb\left(Y_2Y_{12} + Y_{10}Y_4\right) + 2NtY_2Y_{10}\right) \\ & + \sigma^* Sc\left(1 + \delta Y_1\right)^m \exp\left[\frac{-E_1}{1 + \delta Y_1}\right] Y_{11} \\ & + Sc\left(1 + \delta Y_1\right)^{m-2} \exp\left[\frac{-E_1}{1 + \delta Y_1}\right] E_1 \delta \sigma^* Y_9 Y_3 \\ & + Sc\, m\left(1 + \delta Y_1\right)^{m-1} \exp\left[\frac{-E_1}{1 + \delta Y_1}\right] \delta \sigma^* Y_9 Y_3, \qquad Y_{12}(0) = 1. \end{aligned}$$

The stopping criteria for the Newton's method is set as follow:

$$max\left\{|Y_1(p,q)|, |Y_3(p,q)|\right\} < \epsilon.$$

4.4 Analysis of Graphs and Tables

The principal objective is to examine the impact of different parameters on the temperature profile $\theta(\zeta)$ and concentration profile $\phi(\zeta)$. The impact of different factors like magnetic parameter M^2, heat source parameter, B and activation parameter E_1 is observed graphically. Numerical outcomes of the local Nusselt number and local Sherwood number for the distinct values of some fixed parameters are shown in Table 4.1. The rising pattern is found in the Sherwood number due to extending values of Pr and M^2 while the Nu_x decreases. In this table, I is the interval from which the missing conditions p and q can be chosen.

Figure 4.2 reflects the influence of Prandtl number Pr on temperature profile $\theta(\zeta)$. The Pr is the ratio between momentum diffusivity and thermal conductivity. As the values of Pr increase, the thermal diffusivity will show the decreasing behaviour; so, the temperature distribution will be decreased.

Figure 4.3 displays the impact of Eckert number Ec on $\theta(\zeta)$. As the Eckert number specifies the ratio of kinetic energy and enthalpy change of flow, it is clearly observed that the $\theta(\zeta)$ is increased by raising the values of Ec.

Figure 4.4 reflects influence of parameter B on the temperature profile $\theta(\zeta)$. As the heat source parameter increases, there will be an enhancement in boundary layer thickness. So the temperature of fluid will increase as the values of B increase.

Figure 4.5 describes the behaviour of M^2 on $\theta(\zeta)$. The boundary layer thickness is decreased and leads to heat transfer. So the temperature distribution contracts by enhancing the values of M^2.

Figures 4.6 and 4.7 indicate the impact of Nt and Nb on temperature profile $\theta(\zeta)$. As the values of Nt and Nb increase, the temperature profile will also increase. It is because of a temperature gradient. Nano size particles are move towards the

lower temperature because of asymmetry of molecular impacts. The result due to temperature grad the nano size particles experience a force which drives the particles along a temperature gradient towards the lower temperature.

Figures 4.8 and 4.9 indicate the impact of Schmidt number Sc on dimensionless temperature profile $\theta(\zeta)$ and concentration distribution $\phi(\zeta)$. It is the ratio between kinematic viscosity and mass diffusivity. As Sc gets larger, it improves momentum dissipation rate due to which particles concentration decreases. So, the behaviour of temperature distribution is increased and concentration profile is decreased due to accelerating values of Sc.

Figure 4.10 shows the impact of activation energy E_1 on the concentration distribution $\phi(\zeta)$. As there is an increase in the activation energy, there will be decrement is observed in Arrhenius function and promotes the chemical reaction leading to high concentration in boundary layer thickness. It is noticed that as the value of activation energy increases, the concentration profile will also increase.

Figure 4.11 indicates the impact of reaction rate σ^* on the concentration distribution $\phi(\zeta)$. A decrement is noticed in the concentration profile. It is due to of the larger quantity of σ^*. Increment in the districted chemical reaction rate will effectively rise the solubility.

Figures 4.12 and 4.13 describe the impact of B and Nb on the concentration distribution $\phi(\zeta)$. The behaviour of concentration distribution is found to be decreasing while accelerating the values of B and Nb.

Figure 4.14 shows the influence of Eckert number Ec on the concentration distribution. It is clearly noticed that an increase in the number Ec, increases the concentration profile. It is because of Ec, i.e. the ratio between kinetic energy and enthalpy changes, The more the dissipation effect on temperature, the more it is concentrated.

Figures 4.15 and 4.16 indicate the impact of Pr and M^2 on concentration distribution $\phi(\zeta)$. A decrement is noticed in the concentration distribution due to accelerating values of Pr and M^2. It is because of presence of Lorentz force.

TABLE 4.1: Results of $-(Re_x)^{-\frac{1}{2}}Nu_x$ and $-(Re_x)^{-\frac{1}{2}}Sh_x$ some fixed parameters $S = 3.0$, $n = 2.0$, $B = 0.05$, $\epsilon = -1.0$, $Nt = Nb = 0.1$

M^2	Pr	Ec	Sc	δ	E_1	σ^*	$-(Re_x)^{-\frac{-1}{2}}Nu_x$	$-(Re_x)^{-\frac{1}{2}}Sh_x$	I
0.0	0.7	0.1	1.0	0.1	0.01	0.01	-0.539598	1.778136	[-1.6,-0.8]
1.0							-0.542383	1.797075	[-1.6,-0.9]
2.0							-0.541728	1.809996	[-1.5,-0.7]
3.0							-0.540965	1.819798	[-1.4,-0.5]
4.0							-0.540243	1.827689	[-1.2,-0.2]
3.0	1.0						-0.385227	1.811995	[-1.5,-1.0]
	1.5						-0.258176	1.816395	[-0.5,-0.1]
	2.3						-0.170370	1.821173	[-0.4, 0.1]
	7.0						-0.060823	1.830664	[-0.2, 0.4]
	0.7	0.2					-0.549846	1.809740	[-0.8,-0.2]
		0.3					-0.557967	1.809483	[-0.6,-0.1]
		0.4					-0.566090	1.809227	[-0.5,-0.3]
		0.5					-0.574216	1.808971	[-0.3,-0.1]
		0.1	1.5				-0.546364	3.265701	[-1.5,-1.0]
			2.0				-0.549289	4.735878	[-1.4, 0.1]
			2.5				-0.551298	6.214300	[-1.3, 0.1]
			3.0				-0.552758	7.697910	[-1.4, 0.2]
			1.0	0.4			-0.541730	1.810453	[-1.2, 0.2]
				0.5			-0.541731	1.810606	[-0.9,-0.1]
				1.0			-0.541732	1.811367	[-0.9,-0.2]
				1.3			-0.541734	1.811824	[-0.7,-0.1]
				0.1	0.50		-0.541719	1.807769	[-1.5,-1.2]
					1.50		-0.541710	1.805500	[-1.4,-1.0]
					3.00		-0.541705	1.804442	[-1.5,-1.3]
					5.00		-0.541704	1.804168	[-1.3,-1.2]
					0.01	2.0	-0.544975	2.627174	[-1.0, 0.9]
						3.0	-0.545971	2.929907	[-1.3, 0.1]
						4.0	-0.546763	3.194008	[-0.9,-0.1]
						5.0	-0.547417	3.430429	[-0.9,-0.2]

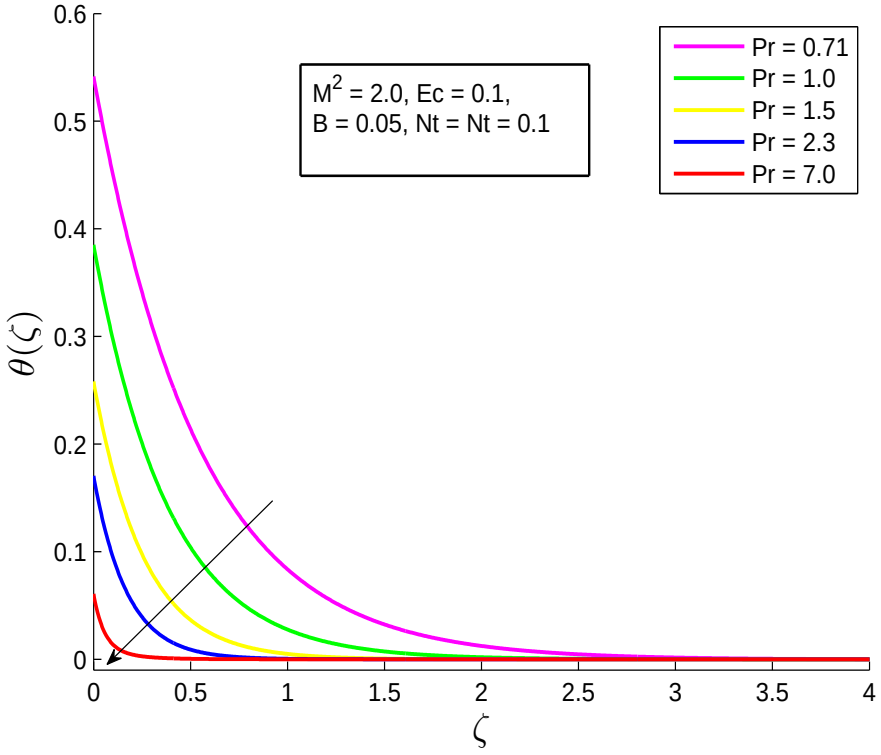

FIGURE 4.2: Impact of Pr on $\theta(\zeta)$.

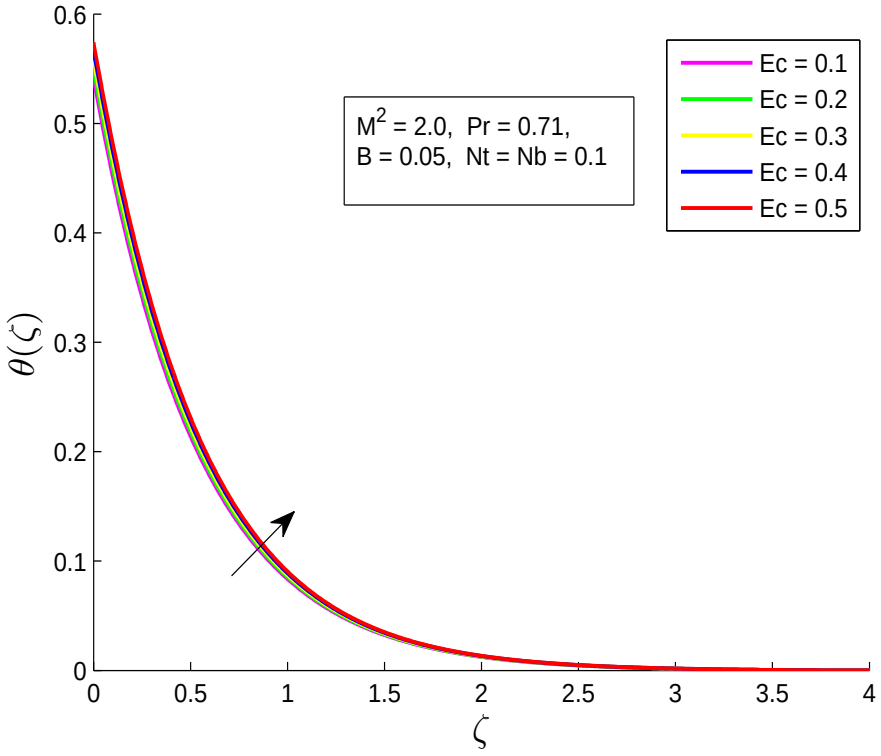

FIGURE 4.3: Influence of Ec on temperature distribution.

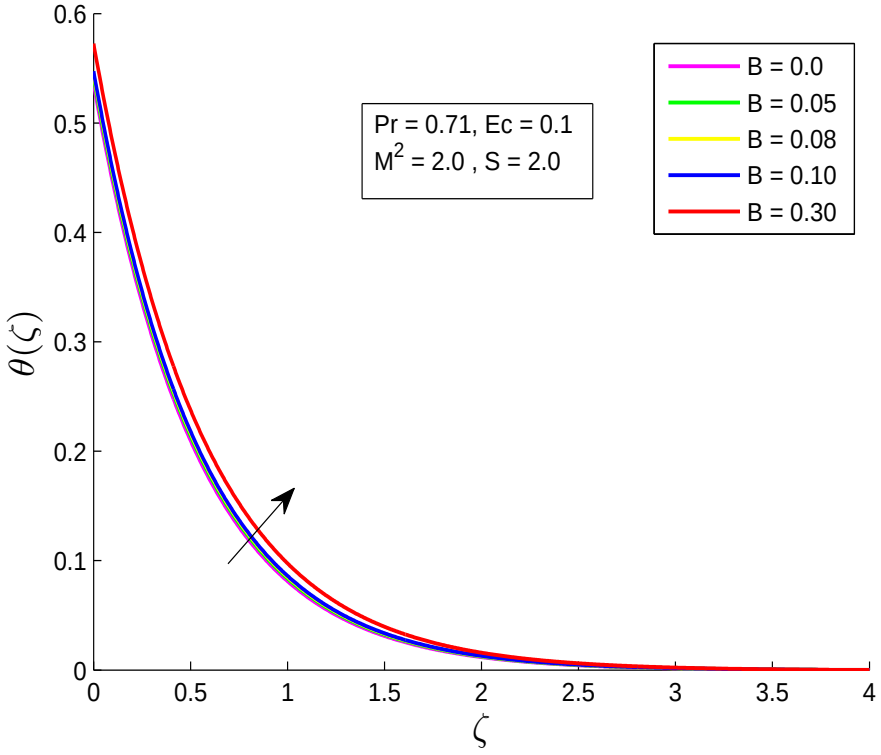

FIGURE 4.4: Impact of B on temperature distribution.

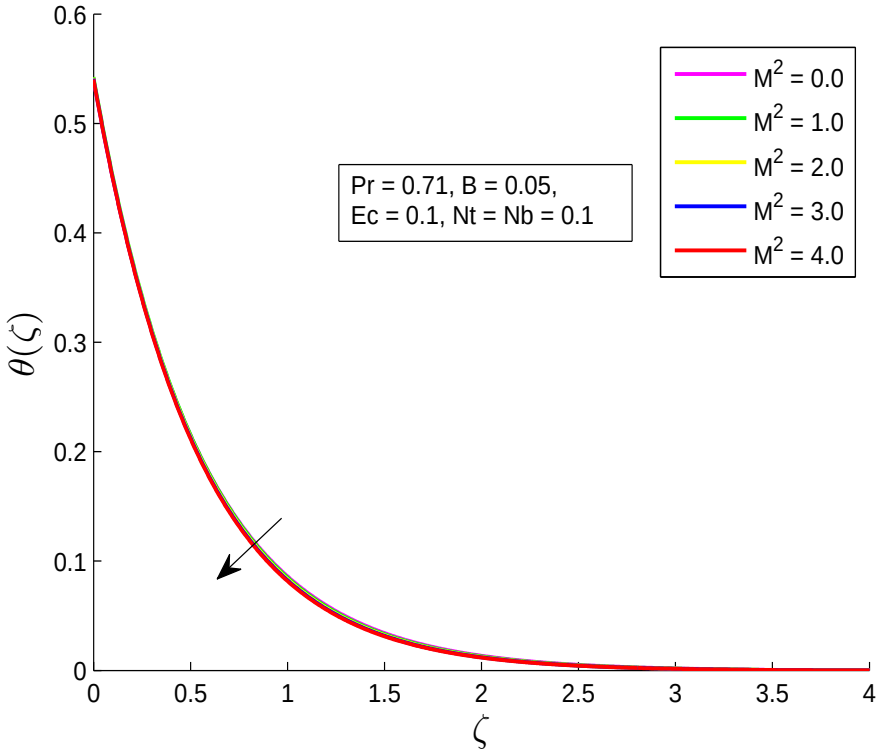

FIGURE 4.5: Influence of M^2 on teperature distribution.

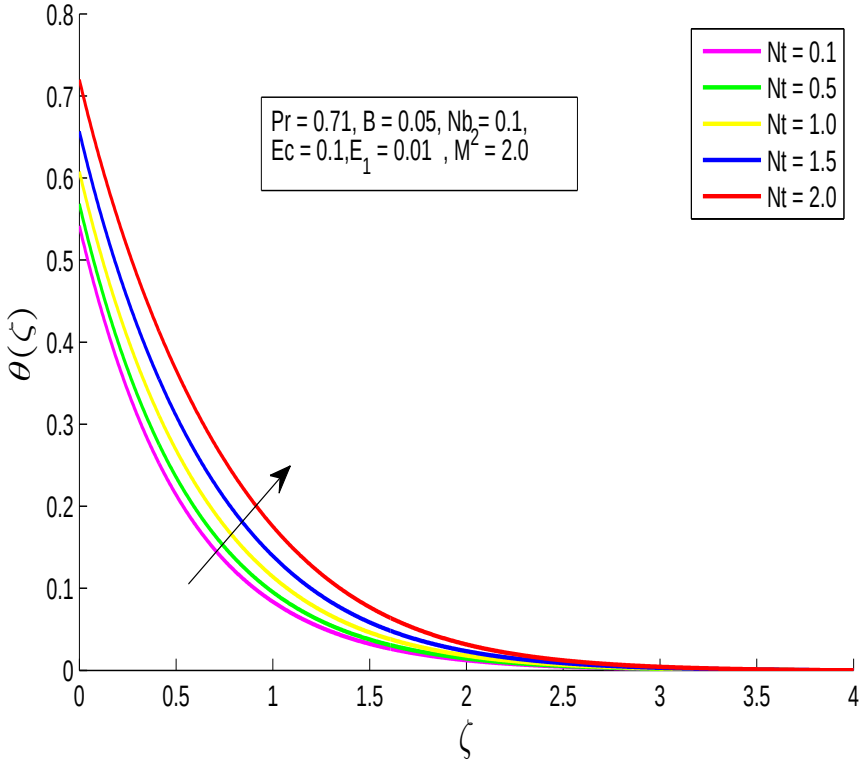

FIGURE 4.6: Impact of Nt on $\theta(\zeta)$.

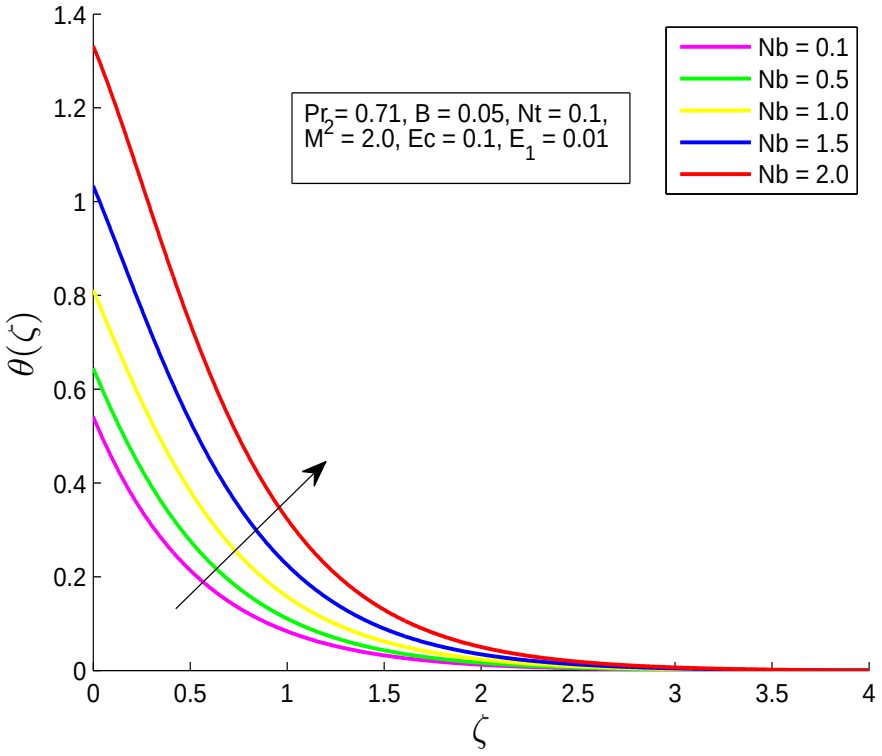

FIGURE 4.7: Impact of Nb on $\theta(\zeta)$.

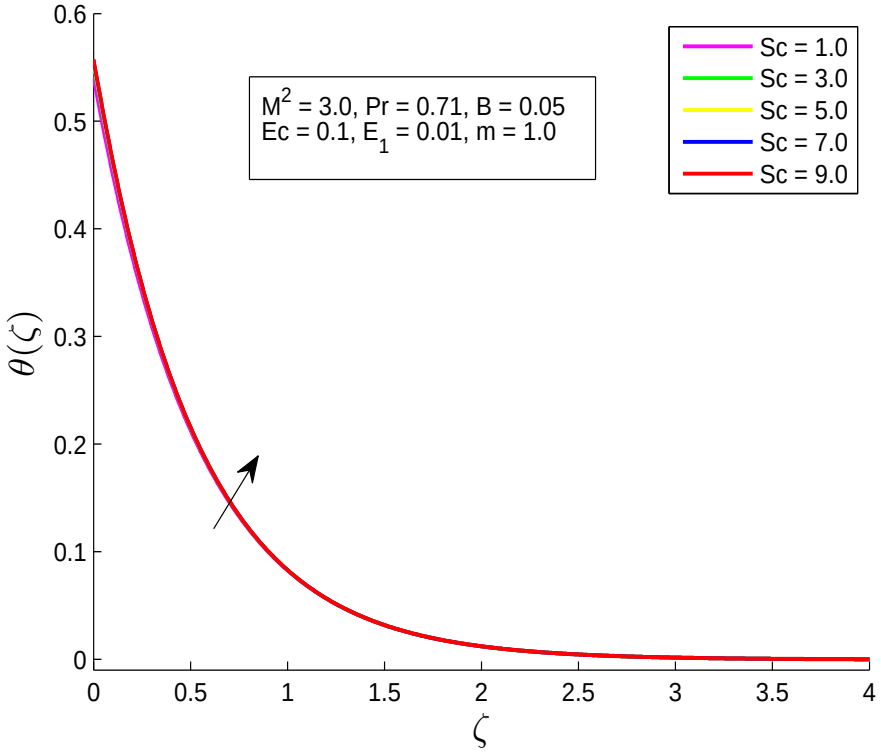

FIGURE 4.8: Impact of Sc on temperature distribution.

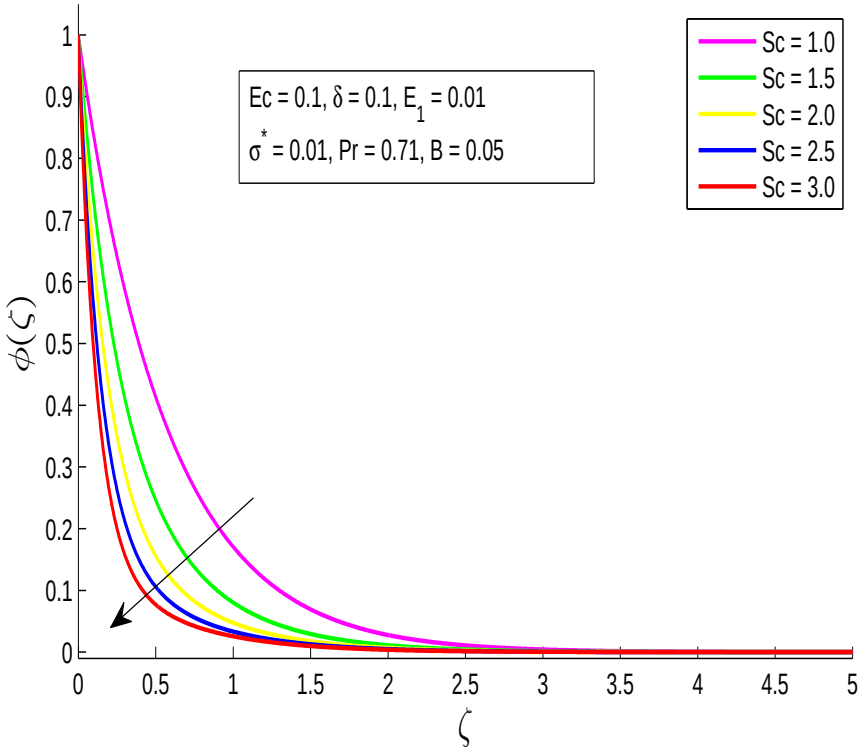

FIGURE 4.9: Impact of Sc on $\phi(\zeta)$.

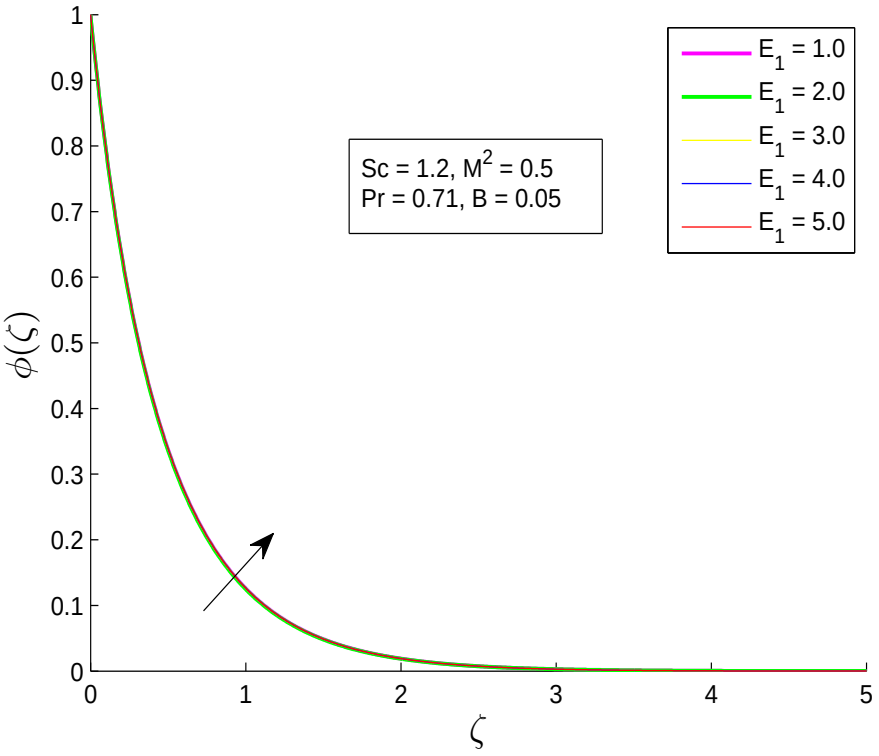

FIGURE 4.10: Effect of E_1 on concentration distribution.

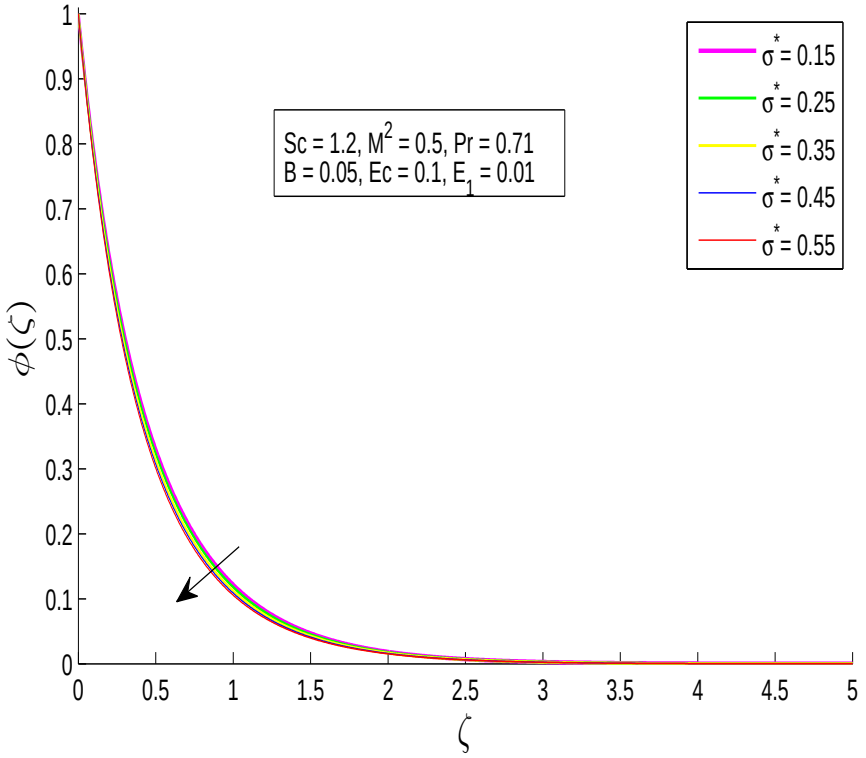

FIGURE 4.11: Influence of σ^* on $\phi(\zeta)$.

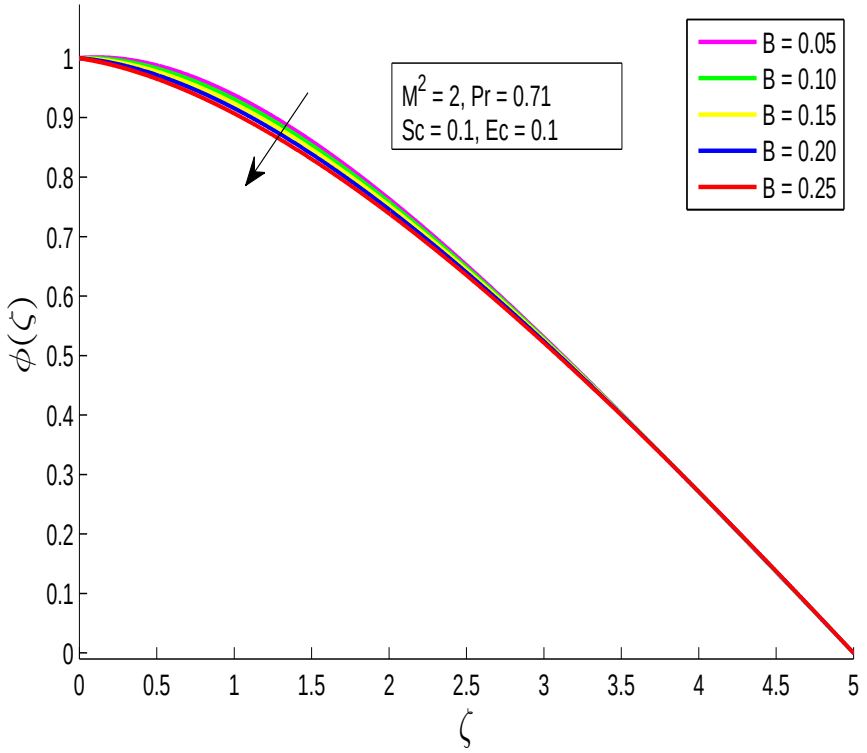

FIGURE 4.12: Influence of B on concentration distribution.

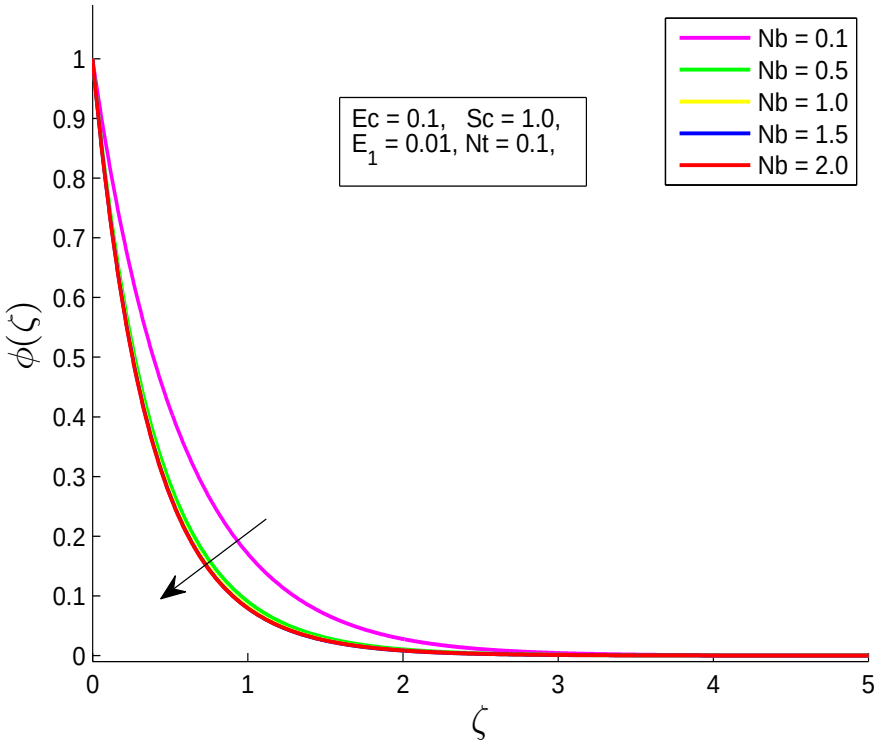

FIGURE 4.13: Effect of Nb on concentration profile.

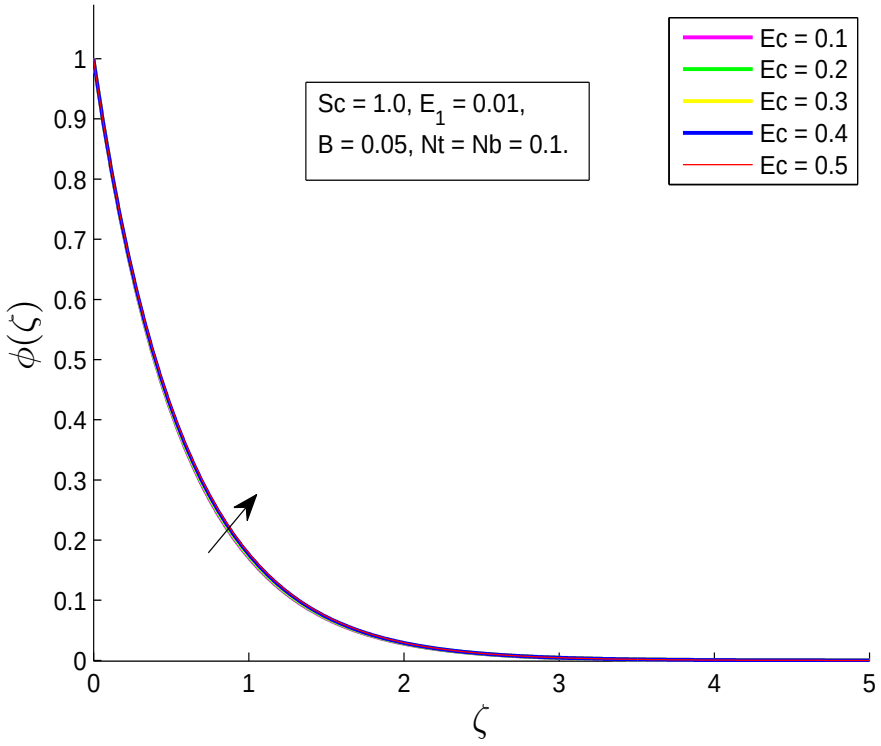

FIGURE 4.14: Impact of Ec on concentration distribution.

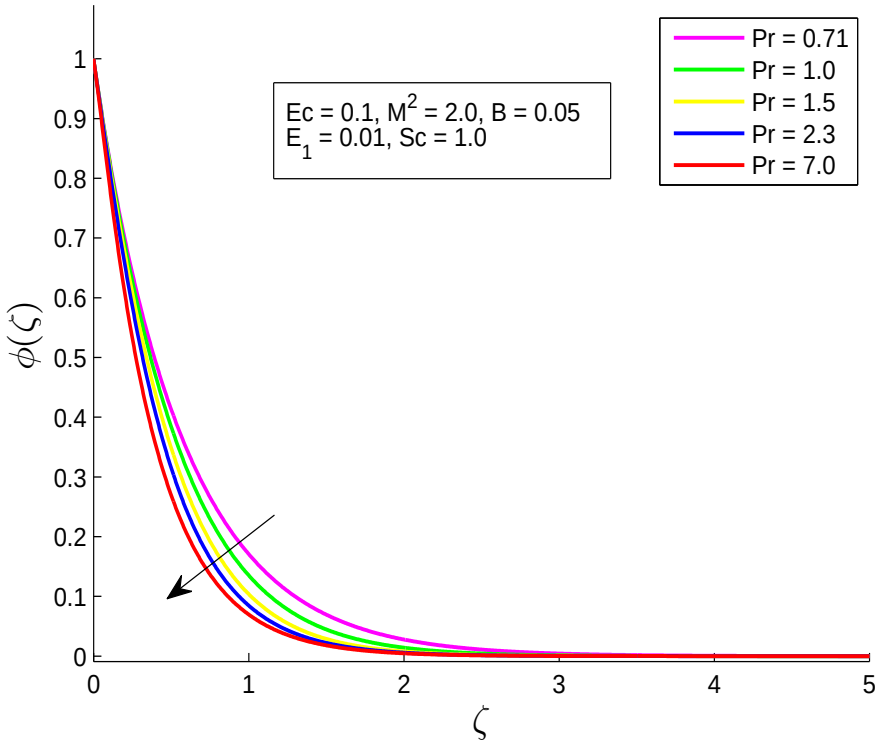

FIGURE 4.15: Influence of Pr on concentration distribution.

Chapter 5

Conclusion

In this thesis, the work of Devi et al. [39] is reviewed and extended with the effect of joule heating effect, Brownian motion, thermophoresis diffusion, chemical reaction rate and activation energy. First of all, momentum, energy and concentration equations are converted into ODEs by using some similarity transformation. By using the shooting technique, numerical solution has been found for the transformed ODEs. For different values of physical parameters, the results are describe in the form of tables and graphs for temperature distribution and concentration profiles. The achievements of the current research can be summarized as below.

- Rising the values of Prandtl number Pr, decrease the temperature profile.
- For enhancing values of Ec and B, the temperature distribution is increasing.
- Increasing values of magnetic parameter M^2, a decrement of temperature profile observed.
- Due to ascending values E_1 the numerical values of local Nu_x increases.
- A decrement is noticed in concentration profile due to increase of Pr number.
- A decrement is noticed in Nusselt number due to ascending values of Sc.
- Due to the ascending values of Nb, the temperature profile increased.

- With a rise in Nb, the concentration profile decreased.
- Due to increasing values of B, a decrement observed in concentration distribution.
- By increasing the values of Pr, the values of local Nusselt and Sherwood numbers are increase.

Bibliography

[1] B. Sakiadis, "Boundary Layer Behaviour on Continuous Solid Surfaces. The Boundary Layer on a Continuous Cylindrical Surface," *American Institute of Chemical Engineering Journal*, vol. 7, no. 3, pp. 467–472, 1961.

[2] L. J. Crane, "Flow Past a Stretching Plate," *Z Angew Math Physics ZAMP*, vol. 21, no. 4, pp. 645–647, 1970.

[3] A. Chakrabarti and A. Gupta, "Hydromagnetic Flow and Heat Transfer over a Stretching Sheet," *Quarterly of Applied Mathematics*, vol. 37, no. 1, pp. 73–78, 1979.

[4] C. K, Chen and Ming-I, "Heat Transfer of a Continuous, Stretching Surface with Suction or Blowing," *Journal of Mathematical Analysis and Applications*, vol. 135, no. 2, pp. 568–580, 1988.

[5] S. Shehzad, Z. Abdullah, F. Abbasi, T. Hayat, and A. Alsaedi, "Magnetic Field Effect in Three Dimensional Flow of an Oldroyd-B Nanofluid over a Radiative Surface," *Journal of Magnetism and Magnetic Materials*, vol. 399, pp. 97–108, 2016.

[6] L. Zheng, J. Niu, X. Zhang, and L. Ma, "Dual Solutions For Flow and Radiative Heat Transfer of a Micropolar Fluid over Stretching/Shrinking Sheet," *International Journal of Heat and Mass Transfer*, vol. 55, no. 25-26, pp. 7577–7586, 2012.

[7] B. Gireesha, B. Mahanthesh, and M. M. Rashidi, "MHD Boundary Layer Heat and Mass Transfer of a Chemically Reacting Casson Fluid over a Permeable Stretching Surface with Non-uniform Heat Source/ Sink," 2015.

[8] M. E. Ali, "On Thermal Boundary Layer on a Power Law Stretched Surface with Suction or Injection," *International Journal of Heat and Fluid Flow*, vol. 16, no. 4, pp. 280–290, 1995.

[9] E. M. Elbashbeshy, "Heat Transfer over a Stretching Surface with Variable Surface Heat Flux," *Journal of Physics D: Applied Physics*, vol. 31, no. 16, p. 1951, 1998.

[10] S. Liao, "A New Branch of Solutions of Boundary Layer Flows over an Impermeable Stretched Plate," *International Journal of Heat and Mass Transfer*, vol. 48, no. 12, pp. 2529–2539, 2005.

[11] R. Bhargava, S. Sharma, H. S. Takhar, and P. Bhargava, "Numerical Solutions for Micropolar Transport Phenomena over a Nonlinear Stretching Sheet," *Nonlinear Analysis: Modeling and Control*, vol. 12, no. 1, pp. 45–63, 2007.

[12] M.-E. Khedr, A. Chamkha, and M. Bayomi, "MHD Flow of a Micropolar Fluid Past a Stretched Permeable Surface with Heat Generation or Absorption," *Nonlinear Analysis: Modelling and Control*, vol. 14, no. 1, pp. 27–40, 2009.

[13] A. Devi and B. Ganga, "Dissipation Effects on MHD Nonlinear Flow and Heat Transfer Past a Porous Surface with Prescribed Heat Flux," vol. 3, no. 1, pp. 1–6, 2010.

[14] P. Vyas and N. Srivastava, "Radiative MHD Flow over a Non-isothermal Stretching Sheet in a Porous Medium," *Applied Mathematical Sciences*, vol. 4, no. 49-52, pp. 2475–2484, 2010.

[15] A. Shahzad, R. Ali, and M. Khan, "On the exact solution for asymmetric flow and heat transfer over a nonlinear radially stretching sheet," *Chinese Physics Letters*, vol. 29, no. 8, p. 084705, 2012.

[16] M. Miklavcic and C. Y.Wang, "Viscous Flow due to a Shrinking Sheet," *Quarterly of Applied Mathematics*, vol. 64, no. 2, pp. 283–290, 2006.

[17] M. Sajid, T. Javed, and T. Hayat, "MHD Rotating Flow of a Viscous Fluid over a Shrinking Surface," *Nonlinear Dynamics*, vol. 51, no. 1, pp. 259–265, 2008.

[18] T. Fang and J. Zhang, "Closed form Exact Solutions of MHD Viscous Flow over a Shrinking Sheet," *Communications in Nonlinear Science and Numerical Simulation*, vol. 14, no. 7, pp. 2853–2857, 2009.

[19] M. Sajid and T. Hayat, "The Application of Homotopy Analysis Method for MHD Viscous Flow due to a Shrinking Sheet," *Chaos, Solitons and Fractals*, vol. 39, no. 3, pp. 1317–1323, 2009.

[20] T. Fang and J. Zhang, "Thermal Boundary Layers over a Shrinking Sheet: An Analytical Solution," *Acta Mechanica*, vol. 209, no. 3, pp. 325–343, 2010.

[21] T. Hayat, S. Iram, T. Javed, and S. Asghar, "Shrinking Flow of Second Grade Fluid in a Rotating Frame: An Analytic Solution," *Communications in Nonlinear Science and Numerical Simulation*, vol. 15, no. 10, pp. 2932–2941, 2010.

[22] F. M. Ali, R. Nazar, and N. M. Arifin, "MHD Viscous Flow and Heat Transfer Induced by a Permeable Shrinking Sheet with Prescribed Surface Heat Flux," *WSEAS Transactions on Mathematics*, vol. 9, no. 5, pp. 365–375, 2010.

[23] N. Noor, S. A. Kechil, and I. Hashim, "Simple Non-perturbative Solution for MHD Viscous Flow due to a Shrinking sheet," *Communications in Nonlinear Science and Numerical Simulation*, vol. 15, no. 2, pp. 144–148, 2010.

[24] K. Bhattacharyya, "Effects of Heat Source/Sink on MHD Flow and Heat Transfer over a Shrinking Sheet with Mass Suction," *Chemical Engineering Research Bulletin*, vol. 15, no. 1, pp. 12–17, 2011.

[25] K. Das, "Slip Effects on MHD Mixed Convection Stagnation Point Flow of a Micropolar Fluid towards a Shrinking Vertical Sheet," *Computers and Mathematics with Applications*, vol. 63, no. 1, pp. 255–267, 2012.

[26] A. Bestman, "Natural Convection Boundary Layer with Suction and Mass Transfer in a Porous Medium," *International Journal of Energy Research*, vol. 14, no. 4, pp. 389–396, 1990.

[27] A. Hamid and M. Khan, "Impacts of Binary Chemical Reaction with Activation Energy on Unsteady Flow of Magneto-Williamson Nanofluid," *Journal of Molecular Liquids*, vol. 262, pp. 435–442, 2018.

[28] S. Jabeen, T. Hayat, S. Qayyum, and A. Alsaedi, "Significance of Activation Energy in Stratified Flow of Tangent Hyperbolic Fluid," *International Journal of Numerical Methods for Heat & Fluid Flow*, 2019.

[29] A. J. Smits, *A Physical Introduction to Fluid Mechanics*. John Wiley New York, 2000.

[30] R. Rajput, *A Textbook of Fluid Mechanics and Hydraulic Machines*. S. Chand publishing, 2015.

[31] R. Bansal, *A Textbook of Fluid Mechanics*. Laxmi publications, 2004.

[32] A. Cengel Yunus and M. Cimbala John, "Fluid Mechanics: Fundamentals and Applications." 2006.

[33] P. A. Davidson and A. Thess, *Magnetohydrodynamics*. Springer Science & Business Media, 2002, vol. 418.

[34] J. N. Reddy and D. K. Gartling, *The Finite Element Method in Heat Transfer and Fluid Dynamics*. CRC press, 2010.

[35] R. W. Lewis, P. Nithiarasu, and K. N. Seetharamu, *Fundamentals of the Finite Element Method for Heat and Fluid Flow*. John Wiley & Sons, 2004.

[36] R. W. Fox, A. McDonald, and P. Pitchard, *Introduction to Fluid Mechanics*, 2006.

[37] M. Gad-el Hak, *Frontiers in Experimental Fluid Mechanics*. Springer Science & Business Media, 2013, vol. 46.

[38] J. Kunes, *Dimensionless Physical Quantities in Science and Engineering.* Elsevier, 2012.

[39] S. A. Devi and J. Raj, "Numerical Simulation of MHD Forced Convective Boundary Layer Flow Past a Stretching/Shrinking Sheet Prescribed with Variable Heat Flux in the Presence of Heat Source and Constant Suction," *Journal of Applied Fluid Mechanics*, vol. 7, no. 3, pp. 415–423, 2014.